AGU PUBLICATIONS

JGR

Journal of Geophysical Research: Oceans

RESEARCH ARTICLE

10.1002/2015JC011424

Key Points:
- Subsurface water properties at midshelf are remarkably similar alongcoast in the northern CCS
- Wintertime (summertime) water properties are strongly (weakly) related to local wind stress
- Freshwater and importance of "remote" winds distinguish the northernmost CCS from its southern counterpart

Correspondence to:
B. M. Hickey,
bhickey@u.washington.edu

Citation:
Hickey, B., S. Geier, N. Kachel, S. Ramp, P. M. Kosro, and T. Connolly (2016), Alongcoast structure and interannual variability of seasonal midshelf water properties and velocity in the Northern California Current System, *J. Geophys. Res. Oceans*, *121*, 7408–7430, doi:10.1002/2015JC011424.

Received 28 OCT 2015
Accepted 20 AUG 2016
Accepted article online 24 AUG 2016
Published online 13 OCT 2016

Alongcoast structure and interannual variability of seasonal midshelf water properties and velocity in the Northern California Current System

B. Hickey[1], S. Geier[1], N. Kachel[1], S. Ramp[2], P. M. Kosro[3], and T. Connolly[4]

[1]School of Oceanography, University of Washington, Seattle, Washington, USA, [2]SOLITON Ocean Services, Inc., Carmel Valley, California, USA, [3]College of Earth, Ocean, and Atmos. Sciences, Oregon State University, Corvallis, Oregon, USA, [4]Moss Landing Marine Laboratories, Moss Landing, California, USA

Abstract Moored sensors were maintained for ~5 years on the northern California Current System (CCS) midshelf. The alongcoast sensor array spanned the area of influence of the plume from the Columbia River, several submarine canyons, as well as a coastal promontory where the equatorward coastal jet frequently separates from the shelf. Upwelling-favorable wind stress magnitude decreases poleward by more than a factor of three over the latitudinal range and shelf width varies by a factor of two. In spite of the alongcoast structure in setting, both seasonal and interannual patterns in subsurface layer water properties were remarkably similar at all sites. Higher in the water column, freshwater forcing was substantial. Because of the near surface freshwater input, seasonal sea surface and subsurface temperatures were almost perfectly out of phase in the northernmost CCS, with a mid water column inversion in winter. Year to year differences in subsurface layer wintertime water properties were similar to spatial and temporal patterns of wind stress variability: little alongcoast structure except in salinity, but pronounced interannual differences strongly related to local wind stress. Summertime wind and subsurface property patterns were the opposite of those in winter: pronounced alongcoast wind stress structure, but little or no alongcoast or interannual variability in water properties, and only a weak relationship to local wind stress. Summertime interannual water property variability, including source waters, was shown to be more consistent with "remote forcing" via larger scale wind stress rather than with local wind stress, particularly in the northernmost CCS.

1. Introduction

Seasonal water properties and alongshelf currents on the continental shelves of an Eastern Boundary System such as the California Current System (CCS) are primarily controlled by seasonal upwelling [*Hickey*, 1979; *Strub et al*., 1987a; *Landry et al*., 1989; *Huyer*, 1990]. In summer, shelf waters below near surface layers are cold and salty; in winter, shelf waters are warmer and fresher. Alongshelf currents are generally equatorward over the shelf and upper slope in summer and poleward in winter (the "Davidson Current"). Direction reversals in the summertime equatorward flow are rare, because the current is primarily baroclinic [*MacFadyen et al*., 2005]. However reversals are common on the inner shelf, where dynamics are frictionally dominated. Undercurrents occur over the continental slope with maximum speeds typically near ~250 m in summer (poleward) [*Hickey*, 1979; *Pierce et al*., 2000], and ~300–500 m in winter (equatorward) [*Werner and Hickey*, 1983; *Kosro*, 2002]. Unlike much of the CCS, the northern CCS (defined as the region north of California, >42°N) has relatively few large coastal promontories to interrupt alongcoast flow and potentially generate local eddies and offshore meandering jets (Figure 1a), a boon to interpretation and analyses.

Seasonal water properties have two primary large-scale sources of variability on northern CCS shelves: the degree of seasonal basin-scale alongcoast advection of shelf and slope water; and the ability of winds (either local or remote) to raise slope water onto the continental shelf. In particular, colder, fresher water is advected equatorward in the upper ~100–200 m of the water column over the slope. Warmer, saltier water is advected poleward in winter via the surface intensified Davidson Current, and in summer and early fall by the subsurface California Undercurrent [*Hickey*, 1979, 1998; *Huyer et al*., 1989; *Thomson and Krassovski*, 2010] providing the bulk of water upwelled onto the northern CCS shelves [*MacFadyen et al*., 2008]. Whatever water is present below the shelf break in late winter (usually nutrient-enriched, colder and saltier than

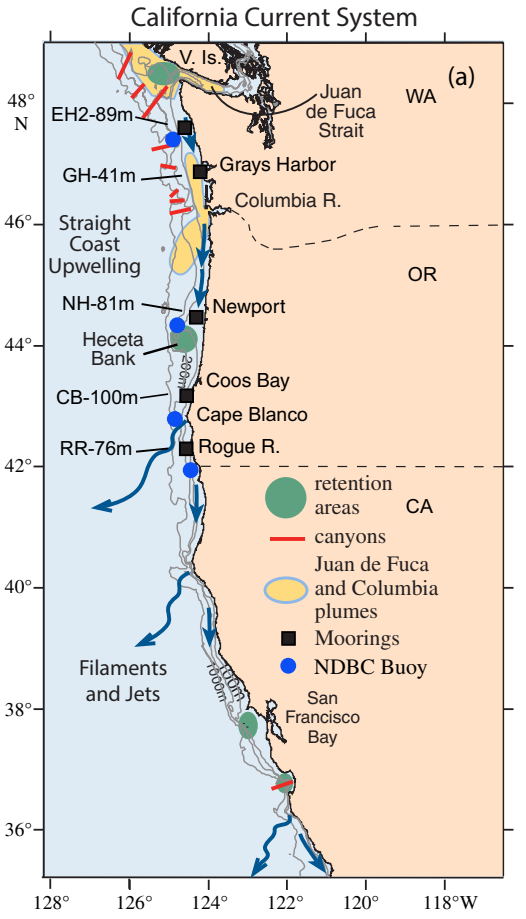

Figure 1a. Locations of moored sensor arrays and environmental setting (submarine canyons, retentive circulation features, typical circulation patterns and freshwater sources) of the arrays within the CCS. Vancouver Island, British Columbia is labeled "V. Is." Bottom depths of moored arrays are listed with each mooring identifier. Adapted from *Hickey and Banas* [2008].

ambient shelf water) is upwelled onto the shelf in spring and summer. The efficiency and depth of upwelling depends on the magnitude, persistence and, if remote wind forcing plays a major role [e.g., *Hickey et al.*, 2006], the alongcoast structure of upwelling-favorable winds along the US west coast, as well as physical characteristics such as local stratification and bottom slope [*Allen et al.*, 1995; *Chapman*, 1983]. The timing and duration of these seasonal patterns can have a large impact on local ecosystems (e.g., the delayed spring transition of 2005 [*Kosro et al.*, 2006; *Kudela et al.*, 2006]).

Inflow from regional estuaries and rivers provides another important source of variability and alongcoast structure in water properties over the northern CCS, impacting temperature and stratification as well as salinity [*Hickey et al.*, 2005; *Mazzini et al.*, 2014]. The majority of the fresher water originates from the Columbia River estuary, typically 20–31.5 psu in its coastal plume. The Columbia provides 77% of all fresh water annually along the coast north of San Francisco [*Barnes et al.*, 1972]. Coastal estuaries such as Grays Harbor, and Willapa Bay, Washington, and Coos Bay, Oregon, input less than 1% of the fresher water in summer to the northern CCS coast [*Hickey and Banas*, 2003]. Freshwater input from coastal rivers has a greater impact (~2–10%) in winter and early spring when rainfall is a maximum (see *Hickey and Banas* [2003], Table 1; *Mazzini et al.* [2014]). A high volume of water originating from the Fraser River in British Columbia, Canada, emanates from the Strait of Juan de Fuca. This fresher water (typically ~30–31 psu) forms a buoyancy-driven coastal current that flows poleward along Vancouver Island in both winter and summer (the "Vancouver Island Coastal Current"). In summer, a portion of this water is entrained into an offshore eddy (the retentive feature offshore of the Strait; see Figure 1a) and moves equatorward along the northern CCS shelf and slope [*Freeland and Denman*, 1982; *MacFadyen et al.*, 2005, 2008].

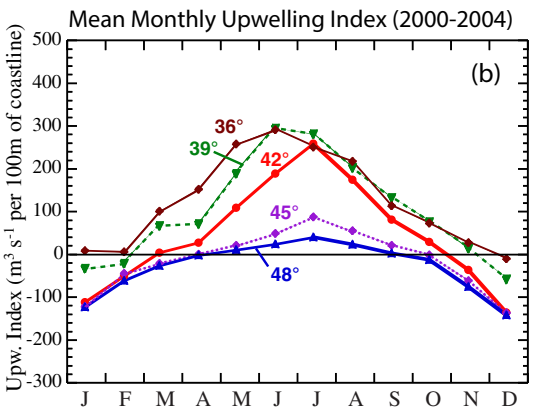

Figure 1b. Seasonal pattern of monthly mean upwelling indices as a function of latitude over the northern and central CCS.

This paper uses a 5 year time series generated from an array of sensors moored at midshelf over an alongcoast distance of about 450 km to describe the alongcoast structure of seasonal and interannual patterns of temperature, salinity, density and alongshelf velocity in the northern CCS (Figure 1a). The physical environment of the moored arrays is highly variable along the coast (Figures 1a and 1b). In particular, moorings are located in bottom depths ranging from 41 to 100 m and at different distances from the coast.

Shelf width varies by a factor of two between the broad, flat Washington shelf (~50 km) and the narrower, steeper northern and southern Oregon shelves (~25 km). Submarine canyons indent the continental slope near the northern end of the moored array, and the two northern sites are also strongly influenced by the plume from the Columbia River in all seasons, by smaller coastal estuaries and rivers in spring and winter [*Hickey et al*., 2005, 2009, 2010], as well as by freshwater from the Strait of Juan de Fuca in summer to early fall. The southern two sites are located on opposite sides of a major coastal promontory, Cape Blanco, where the summertime upwelling jet frequently separates from the coast [*Barth et al*., 2000; *Huyer et al*., 2005]. With respect to forcing mechanisms, upwelling-favorable, large-scale alongshelf wind stress amplitude decreases poleward in summer by more than 70% over the sensor array (Figure 1b) [*Hickey*, 1979; *Hickey and Banas*, 2008]. Our results will show that in spite of these seemingly substantial alongcoast differences, near-uniformity in midshelf water properties below the surface layers is observed along the coast on both seasonal and interannual scales.

The only two earlier studies that addressed large-scale alongcoast structure of shelf properties were limited by having a short duration and also a lack of salinity data (the SUPERCODE moored array [*Strub et al*., 1987a]), or by lack of simultaneous current measurements (multidecadel hydrographic data [*Landry et al*., 1989]). The *Landry et al*. [1989] study, which provides comparison of seasonal cycles for a number of properties including salinity, temperature, nutrients, chlorophyll and oxygen between Washington and Oregon, is a particularly useful resource. The SUPERCODE study provides still very relevant information on the alongcoast structure of seasonal cycles of velocity, wind, sea level and mid water column temperature [*Strub et al*., 1987a] as well as event scale dynamics [e.g., *Denbo and Allen*, 1987] during 1981 and 1982. The data and analyses presented herein are unique in the simultaneous alongcoast measurements of velocity, temperature and salinity as well as the unprecedented longevity of the time series on CCS shelves.

Our overall goal is to provide an analysis of the alongcoast variability, and, further, to ensure that this important and difficult-to-obtain data set and the analysis it has allowed, are made available to the ocean community for understanding monthly mean temporal and spatial variability in interdisciplinary processes such as hypoxia and ocean acidification, for development of new approaches to measurements in upwelling systems, as well as for further testing of next generation models. The analyses will also shed renewed light on the importance of remote forcing to upwelled, summertime water properties on northern shelves as well as the coastwide similarity of upwelled shelf bottom water. The data set and analysis methods are described in section 2. This is followed by presentation of seasonal patterns and their alongcoast structure (section 3.1). Interannual variability and its alongcoast structure are described in section 3.2, followed by a discussion of forcing mechanisms and water sources (section 4), ending with conclusions (section 5).

2. Methods

Data were primarily obtained from moored sensors deployed as components of GLOBEC (Global Ocean Ecosystem) Northeast Pacific and ECOHAB PNW (Ecology of Harmful Algal Blooms Pacific Northwest) field programs. GLOBEC moorings were deployed at four sites from central Washington to southern Oregon (Figure 1a). The moorings were subsurface, with slightly different configurations at each site. Bottom depth ranged from 41 m off central Washington near Grays Harbor (GH) to 100 m at Coos Bay (CB), and 81 and 76 m at the Newport Head (NH) and Rogue River (RR) sites, respectively. Although sensors spanned most of the water column below 10 m from the surface, to allow cross-comparison between sites, only time series at ~20 m (denoted "near surface"), ~35 m (denoted "mid water column"), and ≤10 meters above bottom (denoted "near bottom") were used from each location. At each of these depths, conductivity and temperature data were available in most cases, from a Sea-Bird Electronics (SBE) 37 MicroCAT C-T Recorder, and velocity was available from an upward-looking acoustic Doppler current profiler (ADCP). Because the GH mooring was located much shallower than moorings at the other sites, data from a deeper ECOHAB PNW mooring (EH2, 89 m) deployed ~90 km north of the GLOBEC mooring during 2003 and 2004 were used to illustrate possible bias introduced by using mooring data from a shallower bottom depth (see relative mooring locations in Figure 1a). Use of these data to enable a cross-shelf comparison is justified by our results, which will show that both seasonal and interannual variability of shelf water is large scale (>450 km along the coast). The EH2 mooring was a surface mooring, with a

downward-looking Teledyne RD Instruments 300 kHz Workhorse Sentinel ADCP and an SBE 16*plus* SeaCAT CTD suspended 4 m below a toroidal buoy.

Sampling rates varied on the instruments but were typically 30 min or less. Data were edited for spikes and averaged or decimated to hourly values. These data were low pass filtered to remove higher frequency signals such as tides and internal waves using a cosine-Lanczos filter with a half power point of 46 h, and decimated to 6 h values. Velocity data were rotated to a local isobath coordinate system. Rotation angles were −18 (EH2), −18 (GH), 18 (NH), 13 (CB) and 17 (RR) degrees relative to true north. All data were averaged for each month to produce "monthly means." A mean was only used if the available data exceeded 15 days.

Although the National Data Buoy Center (NDBC) wind buoys are located in some proximity to each mooring site (see locations in Figure 1a), experience dictates that estimating alongcoast gradients from wind buoys distributed along the coast is difficult because physical factors such as variable distance from the coast produce site-to-site differences that can mask the dynamically important alongcoast structure. NCEP Reanalysis winds (National Centers for Environmental Prediction; *Kalnay et al.* [1996]) are derived from large-scale atmospheric pressure and are inherently large scale (∼2.5 degree scale). However they are adjusted by assimilation of measured winds from all available sources (such as NDBC buoys and ships) near and on the coast to provide more accurate shelf coverage. If electing to use synthetic winds such as from NCEP Reanalysis, it is not entirely clear what location, relative to a mooring site, is the best choice for analysis of water property/wind relationships: should winds be extrapolated to the coast to better predict local upwelling over the inner shelf; or to exact mooring locations to better predict cross-shelf flow in the surface Ekman layer; or averaged over the shelf? Of these choices, we have elected to use NCEP Reanalysis winds extrapolated to mooring sites, the motivation being that wind stress used in vertically averaged momentum balance analysis at mooring sites has proven to be a good predictor of local shelf currents in winter [e.g., *Hickey et al*., 1998]. Therefore, 6 h wind speed and direction obtained from the NCEP Reanalysis database were linearly extrapolated to the mooring locations, and used as a proxy for measured winds. At the GH site, where NCEP winds seemed unusually weak in winter, we also included winds extrapolated to a site 40 km offshore of GH (denoted "GH40"), a distance offshore similar to that at the other mooring sites. The NCEP Reanalysis 6 h data were used to compute wind stress, using the drag coefficient of *Large and Pond* [1981]. Wind stress data were then averaged over each month in a manner similar to that of the water property and velocity data discussed above.

To provide larger spatial scale and temporal context information, 14 years of monthly mean upwelling indices (UI) an atmospheric pressure product proportional to large-scale alongshelf wind stress on a 3° grid [*Bakun*, 1975] were acquired from the following website: http://www.pfeg.noaa.gov/products/PFEL/modeled/indices/upwelling/NA/data_download.html.

With the exception of the NH mooring, data were not available in the upper 5 m of the water column. To fill this gap, hourly surface temperature data denoted "sea surface" were obtained from nearby NDBC buoys (see locations in Figure 1a). Data were edited, filtered, and monthly means were obtained as described above.

The numerical model used in this study is an application of the Regional Ocean Modeling System (ROMS) [*Shchepetkin and McWilliams*, 2005] version 3.4 (see complete details and comparison with observations in *Connolly and Hickey* [2014]). The model runs are for the 2005 season, selected for the unusual wealth of observational data to ground-truth model results [*Kosro et al*., 2006; *Connolly and Hickey*, 2014]. Realistic atmospheric forcing and oceanic boundary conditions were used to create a hindcast for 2005. Horizontal grid spacing ranges from 1 km near Juan de Fuca Strait to 5 km near the southeast corner of the model domain (45.5°N to 50°N). Model bathymetry was derived from the gridded Cascadia data set [*Haugerud*, 1999], which has 250 m horizontal resolution. The model has twenty vertical levels and uses the stretching functions of *Song and Haidvogel* [1994]. Minimum depth was set to 3 m in order to avoid drying of grid cells. Bathymetry was smoothed to reduce errors in the calculation of pressure gradients near steep topography. However, the smoothed bathymetry retains the principal canyons in the northern CCS (Figure 1a). At the southern boundary, daily output from the Navy Coastal Ocean Model of the CCS (NCOM-CCS) was used [*Shulman et al*., 2004]. At the northern boundary, which is further north than the extent of the NCOM-CCS model domain, global NCOM was used [*Kara et al*., 2006]. The western boundary of the composite used both NCOM models, transitioning between the two near 48°N. With respect to freshwater, exchange with

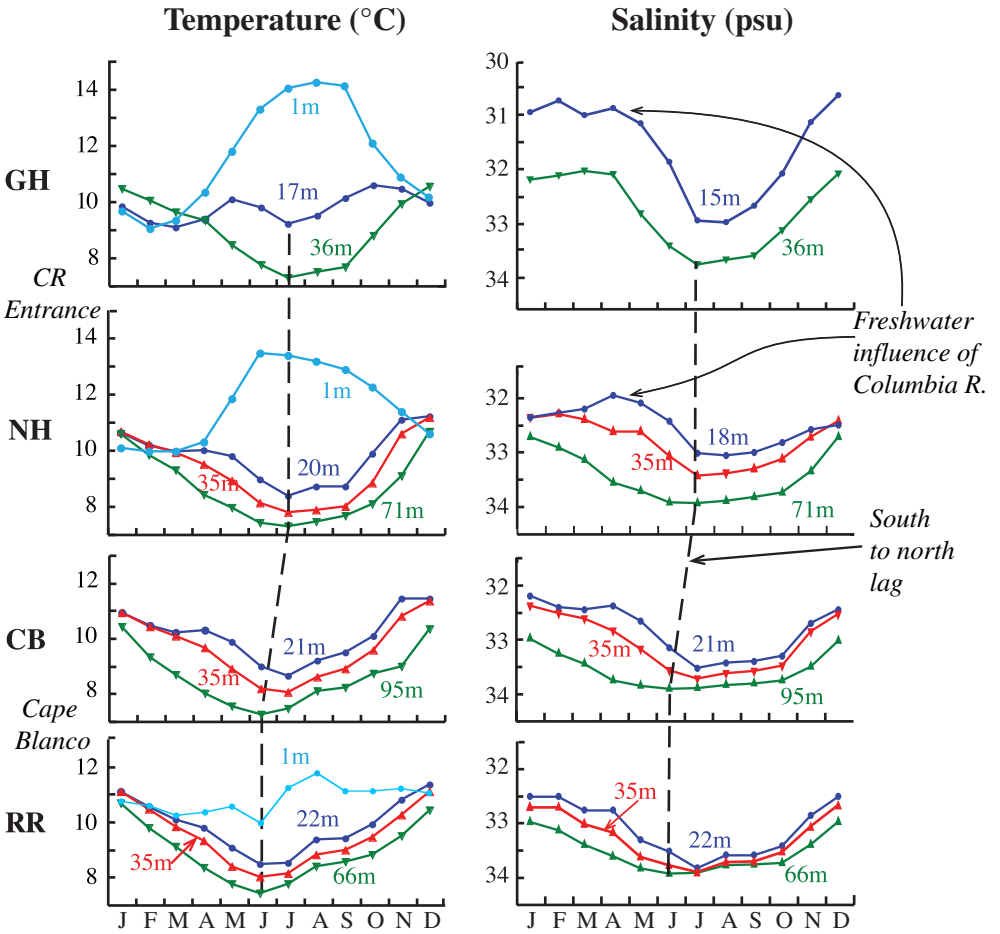

Figure 2a. Mean seasonal patterns of temperature and salinity at selected depths along the northern CCS midshelf. Means were averaged over the period 2000–2004 (2000–2003 at GH; 2001–2004 for surface temperature at NH). Note different salinity range at GH. The dashed lines connect summertime property extremes.

the Juan de Fuca Strait was incorporated by using the model results of *Sutherland et al.* [2011] at the western boundary of the strait. Freshwater input from the Columbia River was not included. In addition to the subtidal fields, amplitude and phase for the K1, M2, O1 and S2 tidal constituents from a tidal model of the northeast Pacific [*Foreman et al.*, 2000] were used on the boundaries. Bulk heat and momentum fluxes [*Fairall et al.*, 2003] were calculated using six-hourly output from a regional atmospheric model [*Mass et al.*, 2003]. In addition to running the model with all features ("Full Model" case), a model run is also shown in which wind speeds over the regional model domain were set to zero ("No Wind" case).

Temperature sections across the Washington shelf and slope used for comparison of model output were obtained from shipboard measurements in the Olympic Region Harmful Algal Bloom (ORHAB) and ECOHAB PNW studies using a calibrated SeaBird CTD. Data were edited and binned in 1 m intervals.

3. Results

3.1. Seasonal Patterns and Their Alongcoast Structure

3.1.1. Water Properties

The seasonal pattern of salinity is similar at all depths and at all sites: water is saltier in summer and fresher in winter (Figure 2a). This is the signature of the seasonal upwelling and downwelling that occurs due to seasonal changes in the direction of large-scale wind stress [*Landry et al.*, 1989; *Huyer et al.*, 2007]. Remarkably, and in spite of the alongcoast 3-fold gradient in summertime wind stress as well as other environmental differences, the salinity of upwelled near bottom water is virtually the same (~33.9 psu, standard

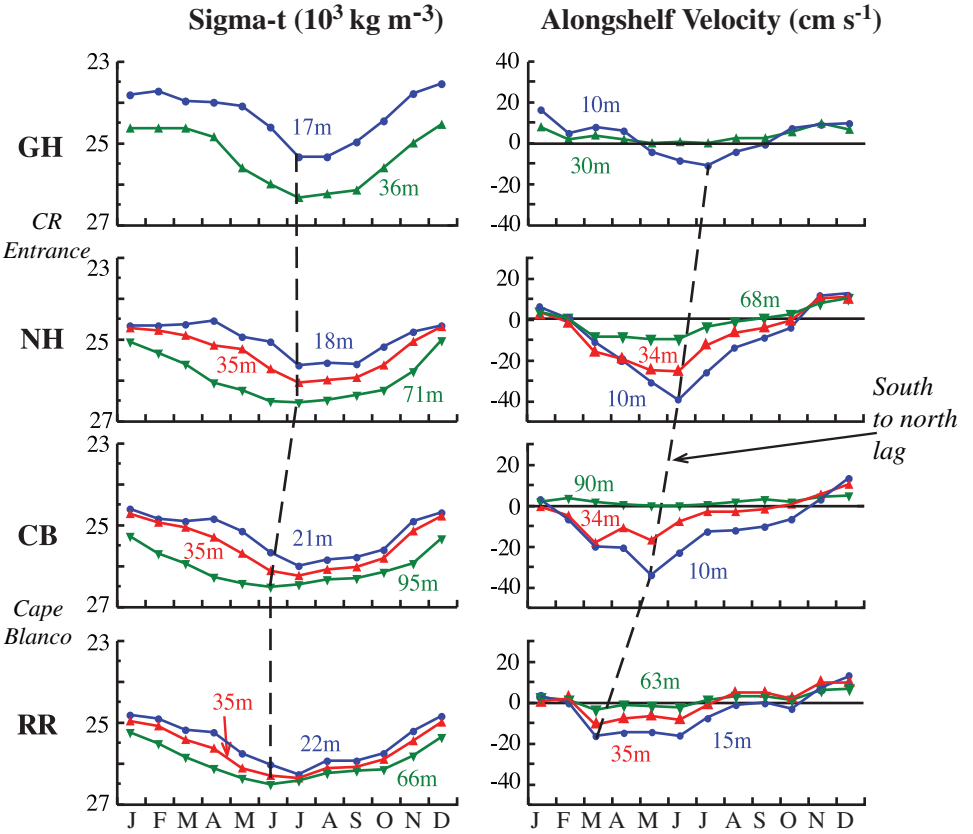

Figure 2b. Mean seasonal patterns of density and alongshelf velocity at selected depths along the northern CCS midshelf. Velocity data were rotated to a natural isobath reference frame, positive poleward. Means were averaged over the period 2000–2004 (2000–2003 at GH). Note different velocity range at GH. The dashed lines connect summertime property extremes.

deviation (σ) = 0.06 NH, 0.06 CB, 0.10 RR) at all sites south of the Columbia River entrance. Near bottom salinity is slightly fresher (~33.7 psu, σ = 0.06 GH) at the site north of the Columbia River entrance: this is likely due primarily to the shallower mooring depth (see section 3.1.3) rather than to poleward-tending plumes from the Columbia River—these plumes are generally surface trapped in summer [*Hickey et al.*, 2005]. The saltiest water occurs generally in early to mid summer at every site. The month in which the most saline water is observed has a south to north lag of ~1 month between the southern and northern sites, with the maximum change in timing between southern and central Oregon.

The seasonal pattern of temperature below the near surface layer is similar in most respects to that of salinity: the lower water column is coldest in summer and warmest in winter at all sites (Figure 2a). Warmest and coldest temperatures occur in phase at all depths below the near surface layers, with the exception of the CB site, where the coldest water occurs later above the near bottom layer. The average coldest near bottom temperature is ~7.3°C at all sites except RR where it is 7.4 (σ = 0.09, 0.12, 0.24, 0.27 at the 4 stations, from north to south). Maximum winter near bottom mean temperature is ~10.7°C at NH and RR (σ = 0.39, 0.63 at NH and RR, respectively), but slightly colder (10.4–10.5°C, σ = 0.66, 0.62 at CB and GH, respectively) at the two other sites. As with maximum summer salinity, the seasonal appearance of the coldest water has a south to north lag of ~1 month between the southern and northern sites.

Near surface salinity and temperature are strongly influenced by buoyant plumes from the Columbia River even at depths of 15–35 m (see typical Columbia plume location in Figure 1a). The freshwater plume is present north of the river mouth in winter, but typically occurs both north and south of the river mouth in spring and summer [*García-Berdeal et al.*, 2002; *Hickey et al.*, 2005, 2009, 2010; *Mazzini et al.*, 2014]. Coastal rivers off both Washington and Oregon can contribute to the freshwater input especially in winter and early spring. Although individually they have at least an order of magnitude smaller volume than the Columbia, cumulatively they can account for up to 2% of the total volume [*Hickey and Banas*, 2003]. Thus, the water

column above 35 m is usually fresher at both the central Washington (GH) and central Oregon (NH) sites throughout the year with the effects particularly pronounced at GH. This mooring site is located in the direct path of poleward–directed Columbia plumes from fall through spring and early summer (Figure 1a). In late spring, when freshwater plumes from the Columbia are more frequently oriented southwest across the Oregon shelf and slope, fresher water is also observed at NH on the shelf south of the river mouth. This produces a seasonal salinity minimum in April at 18 m off Oregon, the freshest water of the year at that depth. Freshwater effects are also observed in the near surface layers in late spring off southern Oregon (CB) and to a lesser degree at the Rogue River (RR) site.

Plumes from the Columbia (year round) and other coastal rivers (primarily winter and early spring) have a greater effect on the seasonal pattern of temperature than that of salinity over the shelf: effects can be both direct, due to plume water temperature, or indirect, due to plume effects on stratification. Thus the freshwater causes patterns of sea surface (∼1 m) and near bottom temperature to be almost perfectly out of phase at the two northernmost stations (Figure 2a, and see also *Landry et al*. [1989]). This behavior occurs because river plumes in the northern CCS are warmer than ambient coastal waters from spring to early fall, and colder than ambient waters in winter [*Hickey et al*., 1998]. Plume seasonal ranges exceed those of ambient waters in part due to the greater seasonal warming (cooling in winter) of the shallow coastal estuaries; and, in part due to the strong summertime stratification that allows the near surface coastal water column to retain heat. In winter, freshwater plumes cause a thermal inversion in the water column both north and south of the Columbia River entrance (GH and NH) as well as at the site near the Rogue River (RR): near surface waters are colder than those deeper in the water column (see also *Landry et al*. [1989], Figure 1.5). The volume of the Columbia River plume is so great that the thermal inversion covers almost the entire Washington shelf (see property atlas for Pacific Northwest coastal waters [*McGary*, 1971]).

At most mooring sites near surface waters warm slightly in spring as they become fresher, and this effect diminishes equatorward in concert with the equatorward reduction of freshwater discharge (Figure 2a). Off the central Washington coast (GH) the warmest sea surface temperatures occur in summer (∼14°C), when near bottom water is coldest. Off central Oregon (NH), warmest temperatures in near surface layers occur earlier in the season due to additional stratification associated with the warmer Columbia plume. Thus Washington's shallow sea surface waters are warmer in summer and colder in winter than Oregon's sea surface waters.

The seasonal pattern of density, like those of temperature and salinity, is similar at all sites, with densest water in summer and lightest water in winter at all depths and at all sites (Figure 2b). Comparison of the salinity and temperature (Figure 2a) and density (Figure 2b) time series shows that density stratification is dominated by salinity rather than temperature; e.g., the north-to-south decrease in stratification from spring to summer mimics a similar increase in salinity gradients, but not in temperature gradients. The near surface layers display freshwater effects in spring and this effect diminishes equatorward. As with temperature and salinity, a south to north lag of the appearance of the densest water is observed in summer. The overall effect of freshwater on stratification in the northern CCS is to produce a latitudinal gradient, with decreasing stratification equatorward.

3.1.2. Alongshelf Velocity

In general, mean alongshelf velocity is equatorward in summer and poleward in winter at all sites, consistent with previous studies [*Hickey*, 1979; *Strub et al*., 1987a]. However, the alongshelf velocity pattern has much greater alongcoast structure than water properties (Figure 2b). The variability is expressed most strongly in the equatorward flow observed in summer at all sites: the onset of equatorward flow as well as its duration and its magnitude differ noticeably between sites. The summertime equatorward flow is the signature of the "coastal jet" that develops in the upwelling season over the shelf in most eastern boundary systems. The coastal jet moves across the shelf during the upwelling season [e.g., *Allen et al*., 1995] and its location varies with forcing and stratification. With a single mooring it is impossible to definitively separate variation in the speed of the coastal jet from its cross-shelf movement. Some of the observed variability is likely due to the location of the jet and its seasonal movement. For example, flow is particularly weak at the central Washington site (GH)—this site is in relatively shallow water; hence it is likely located well shoreward of the equatorward seasonal coastal jet. Moreover, springtime flow on the Washington midshelf at this nearshore site is impacted by poleward flowing plumes from the Columbia River [*Hickey et al*., 2005] (see salinity

in Figure 2a). As discussed in section 3.1.3 below, much stronger equatorward flow, peaking earlier in the year (April–July) is typical of deeper sites off the Washington coast).

Weaker equatorward flow also occurs at the southern end of the sensor array, at the site situated downstream of Cape Blanco (RR). The coastal jet separates from the coast at Cape Blanco [*Barth et al*., 2000] and this site is frequently located inshore of the separation zone [*Ramp and Bahr*, 2008]. The strongest equatorward flow is observed off central Oregon (NH). Coastal Ocean Dynamics Applications Radar (CODAR) maps of surface currents indicate that NH is located, as planned, near the core of the summer coastal jet [*Kosro*, 2005]. As with temperature and salinity, a south to north lag occurs in the maximum equatorward velocity. The large lag between the central Oregon and central Washington sites is likely due to the shallower location of the Washington mooring (see below).

The most persistent mean poleward undercurrent on the shelf is observed at CB. This result is likely because the deeper mooring depth (~100 m) provides closer proximity to the California Undercurrent on the adjacent slope. Velocity shear is weaker at the southernmost site (RR) than at the other Oregon sites.

3.1.3. Cross-Shelf Patterns on the Washington Coast

The central Washington mooring (GH) is located in a shallower bottom depth than the other moorings, just seaward of the inner shelf (~41 m versus ~76–100 m). In spite of the shallower location, average near bottom minimum temperature at the shallower site is indistinguishable from near bottom temperature at the other sites (Figure 2a). Near the surface, however, both salinity and temperature are clearly affected not only by the shallow location, but also by proximity to buoyant plumes from the Columbia River.

To evaluate differences in seasonal patterns on the Washington shelf that might be attributed to the shallower mooring depth, temperature, salinity and velocity data at the shallower site (GH) were compared with data from 2003 and 2004 for a deeper site (EH2, ~90 km north of GH) (Figure 3a). Near bottom water is colder and saltier at the deeper site, consistent with typical cross-shelf patterns in bottom water (see e.g., *Hickey et al*. [2013], Figure 6). The near surface water, on the other hand, is fresher and warmer at the deeper site, because it is located farther seaward of the region impacted directly by coastal upwelling (typically ~10 km, one Rossby radius of deformation). Near surface layers at the deeper site are also more influenced by equatorward advection of fresher, warmer water from the Juan de Fuca region [*MacFadyen et al*., 2005].

Summertime bottom water properties at the deeper Washington site (EH2, 89 m) and those at a slightly shallower bottom depth off Oregon (NH, 81m) show similar seasonal patterns. However, near bottom water is colder at the more northern site (average difference ~0.4°C, Figure 3b) and occurs earlier in at least one of the two years with available data; salinities are similar at the two sites (Figure 3b). This alongcoast structure is consistent with eight pairs of near-simultaneous CTD sections across the central Washington and Oregon shelves (<2 days between sampling of the two sections) obtained in several years and different seasons during the River Influences on Shelf Ecosystems study [*Hickey et al*., 2010] (not shown; also, see higher nitrate, an indication of colder water to the north as shown in Figure 6 of *Hickey et al*. [2010]).

Alongshelf near surface velocity differs between the shallow and deep Washington sites more dramatically than water properties (Figure 3a). In particular, the equatorward flow is much stronger at the deeper site and occurs earlier, consistent with historical studies on the Washington shelf (see *Hickey* [1989], Figure 2.9). The seasonal pattern at the deeper Washington site is similar to that off northern Oregon in a similar bottom depth (81 versus 89 m) (Figure 3b). However, the maximum speed of the near surface velocity is less than that off central Oregon (~30 versus ~45 cm s^{-1}), where the shelf is much narrower.

3.2. Interannual Variability and Its Alongcoast Structure

3.2.1. Water Properties

Time series of monthly mean temperature, salinity and density over the 5 year record show that although the seasonal pattern is dominant at all depths and locations, year-to-year variability is pronounced (Figures 4a and 4b). At depths below direct freshwater influences (>20 m at the southern sites, >35 m at northern sites in winter) year to year trends in salinity, temperature and density are similar at all four sites in both summer and winter. Variability is similar throughout the middle and lower water column at all sites. An exception occurs in salinity at NH, where minimum salinity occurs later higher in the water column, a result of freshwater input from the Columbia River. In summer, maximum salinity and minimum temperature were roughly constant from 2000 to 2003 (near bottom summertime salinity range ≤0.2 psu; temperature range ≤0.4°C) at each site, but freshened in summer 2003 at some sites and warmed and freshened in

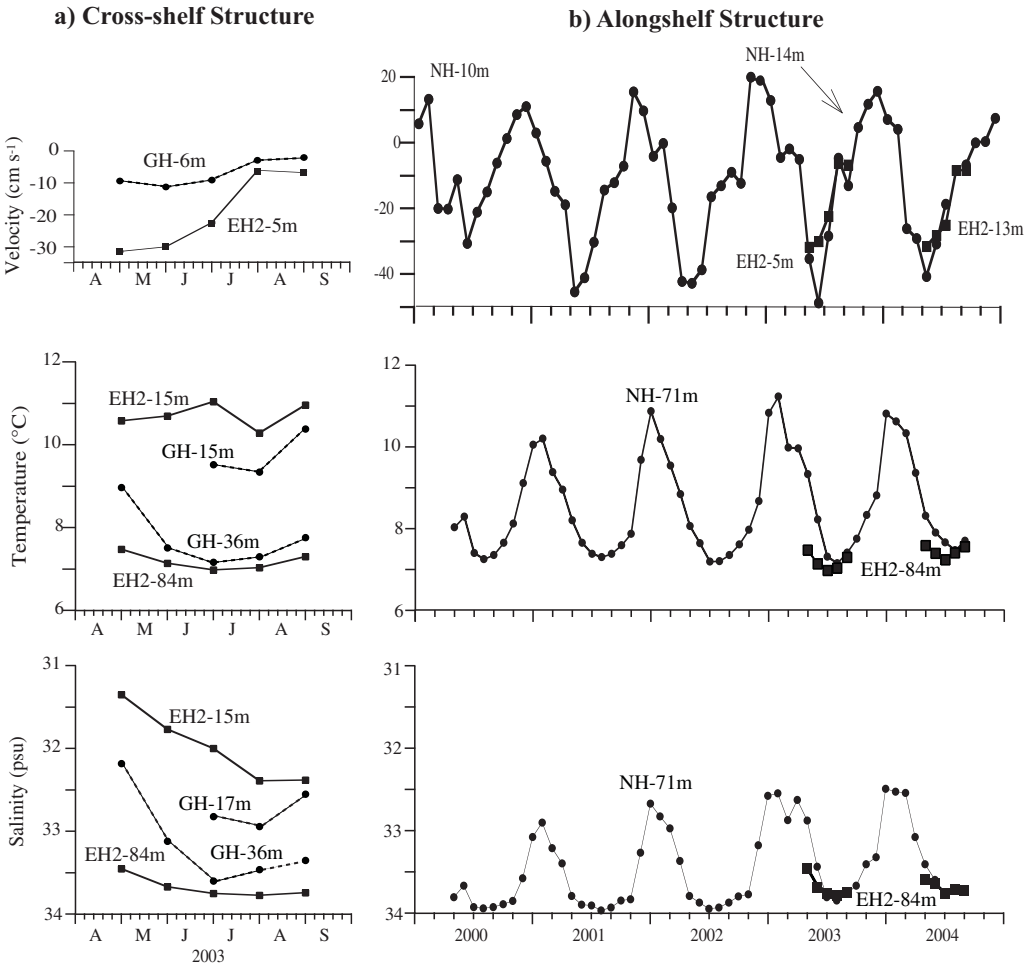

Figure 3. (a) Cross-shelf comparison of seasonal near surface alongshelf velocity, temperature, and salinity at selected depths at two sites on the Washington shelf, one at the shoreward edge of the midshelf (GH, 41 m bottom depth), the other at midshelf (EH2, 89 m bottom depth). Mooring locations are shown in Figure 1a. (b) Alongcoast comparison of seasonal near surface alongshelf velocity as well as near bottom temperature and salinity from sensors in similar mooring depths off the central Washington (EH2, 89 m) and central Oregon (NH, 81 m) coasts.

2004 at all sites where data are available. The similarity in trends in summer extends upward in the water column to ~20 m at the two southern sites as well as to the 18 m temperature at the central Oregon site (NH). In winter, at every site, water generally warmed and freshened each year between 2000 and 2002, then cooled and became saltier in winter 2003 at most sensor depths (near bottom wintertime salinity range 0.7 psu, without GH, the shallower site; 1.7 psu with GH; temperature range 1.9°C with or without GH) (see dashed blue curve in Figure 4a).

Although wintertime water properties differ noticeably from year to year over the region, water upwelled onto the shelf the following season appears to retain no memory of the preceding winter's water properties; i.e., summertime near bottom properties were uncorrelated with property extrema in the prior winter. For example, in summer, near bottom water was colder and saltier for 4 years, but warmed and freshened in summer 2004; whereas the maximum temperature of the preceding winter warmed each year (up to ~1.5°C over the first 3 years), then cooled by ~0.5°C in winter 2003 (Figure 4a).

3.2.2. Alongshelf Velocity

In general, alongshelf velocity displays much more spatial and interannual variability than water properties (Figure 4b) and shows little relationship either to water properties or alongshelf wind stress. For example, the summertime equatorward flow at the site just north of Cape Blanco (CB) increased in speed each year through 2003 and maintained its increased speed in 2004. The overall increase was about a factor of two in

near surface layers. This increase was particularly surprising since upwelling-favorable wind stress at that latitude *decreased* between 2001 and 2004 by about a factor of 0.6 (Figure 5a). At the site just south of Cape Blanco (RR) speeds in the equatorward flow decreased between 2001 and 2002 then increased by a factor of ~2 from 2002 to 2004. Thus a pronounced latitudinal gradient in alongshelf velocity occurred at the two sites on either side of Cape Blanco after 2001. At the central Oregon site (NH) maximum monthly speeds in the summertime equatorward flow increased by a factor of ~1.5 between 2000 and 2001 then leveled off in 2003 to about the same magnitude as at the southern Oregon site (CB) for the remainder of the record. The weak coherence of the seasonal equatorward flow along the coast in comparison to the coherence of water properties, as well as the lack of a relationship to wind stress are likely due in part to cross-shelf movement of the coastal jet as discussed in section 3.1.2.

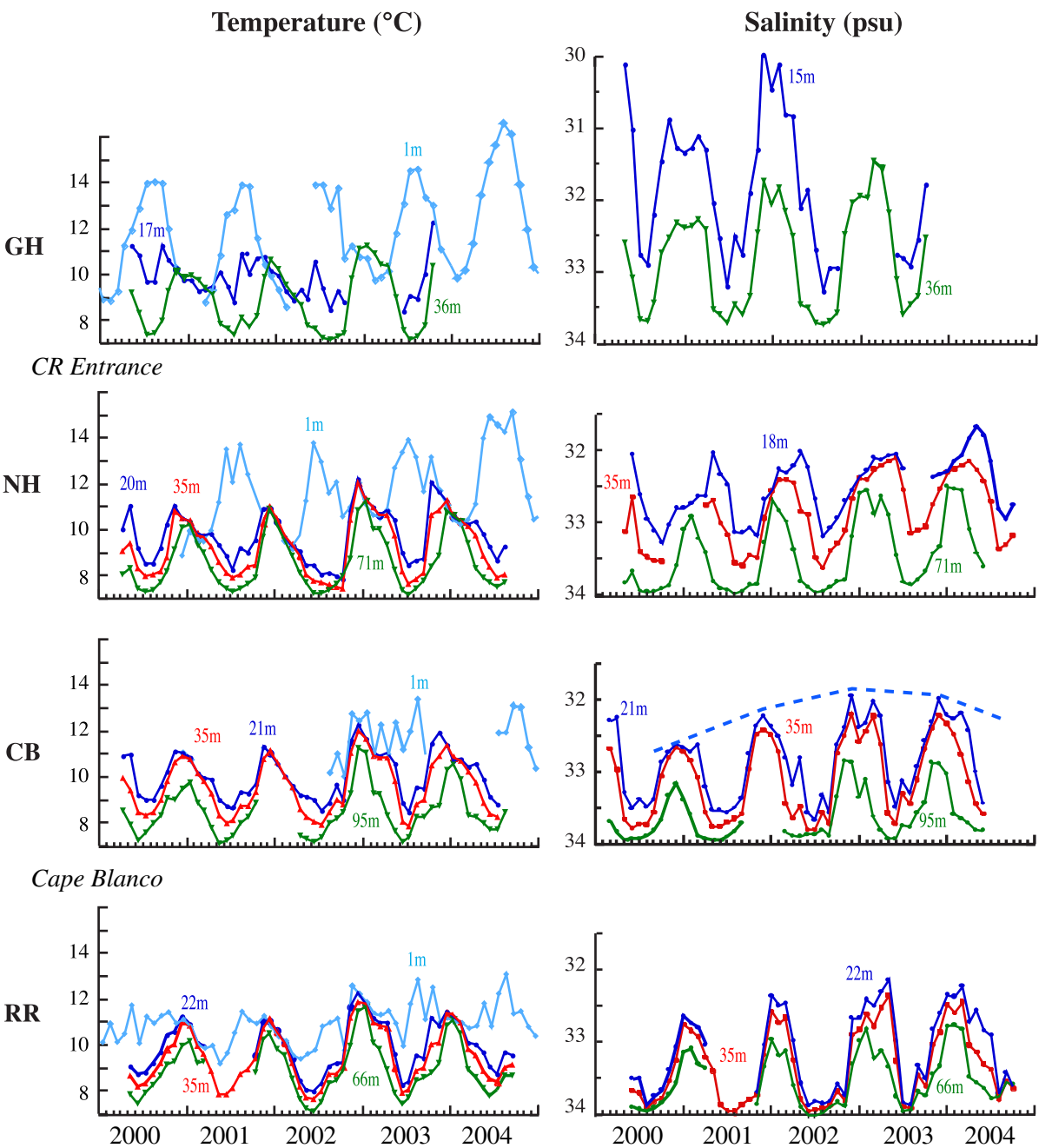

Figure 4a. 5 year record of temperature and salinity at selected depths at sites along the northern CCS midshelf. Note that the GH site is shallower and closer to the inner shelf than the other sites. The dashed blue line on the salinity time series emphasizes the interannual wintertime trends.

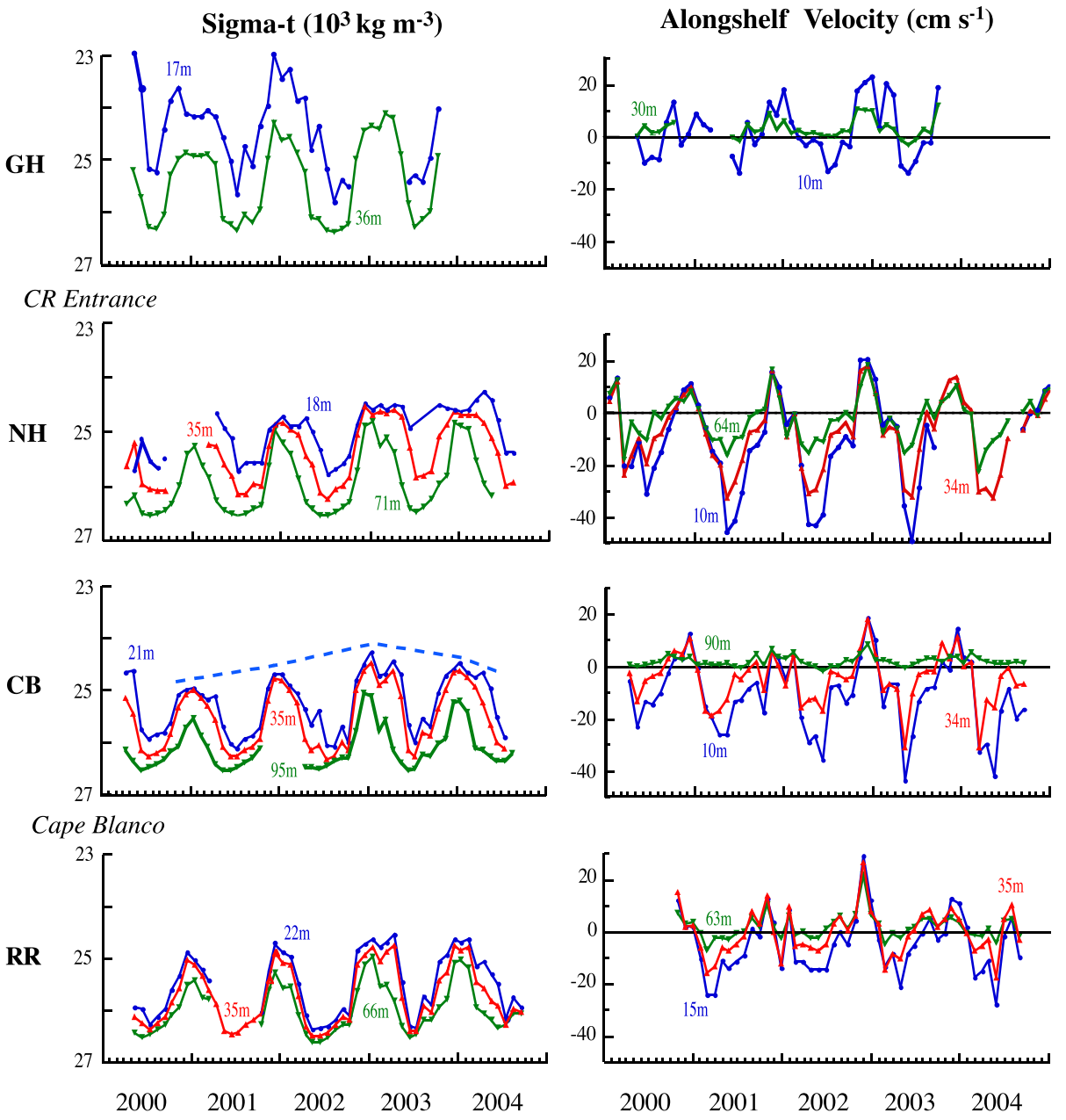

Figure 4b. 5 year record of density and alongshelf velocity at selected depths at sites along the northern CCS midshelf. Note that the GH site is shallower and closer to the inner shelf than the other sites. The dashed blue line on the density time series emphasizes the interannual wintertime trends.

4. Forcing Mechanisms and Water Sources

This paper presents a 5 year time series of water properties and velocities at midshelf in an active eastern boundary upwelling region along the US west coast, with the primary goal of examining alongcoast structure. The seasonal patterns of temperature and salinity below the near surface layers are consistent with being primarily driven by summertime uplifting of isopycnals in response to upwelling-favorable winds and wintertime depression in response to downwelling-favorable winds [*Huyer*, 1983; *Landry et al.*, 1989]. Water properties have similar seasonal and interannual patterns of variability along the coast, and, perhaps more surprising, similar extreme properties at all depths below the direct influence of freshwater, in spite of the variation in shelf width and slope, stratification, location of topographic features such as submarine canyons and coastal headlands, and wind forcing which varies substantially over the study area. The relationship between

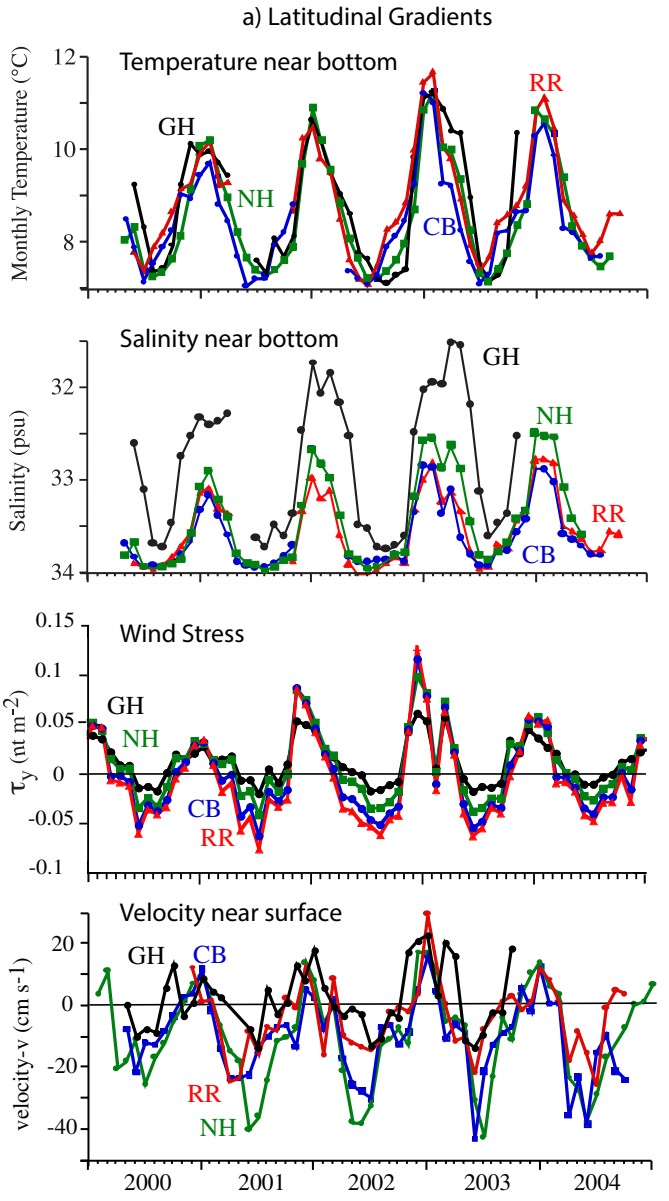

Figure 5a. Alongcoast comparison of near bottom water properties, alongshelf wind stress and near surface alongshelf velocities for the 5 year record. Note that the GH site is shallower and closer to the inner shelf than the other sites.

water property patterns and possible forcing mechanisms, including wind stress, source water variability and remote forcing, are explored in more detail in the sections that follow.

4.1. Wind-driven Upwelling

4.1.1. Wind Stress Patterns and Variability

The alongshelf wind stress has pronounced interannual variability over the 5 year record and the variability is similar along the coast in both seasons (Figure 5a). However, both alongcoast structure and degree of variability from year to year differ between winter and summer. In winter, maximum downwelling-favorable wind stress in the period sampled varies from year to year but there is no consistent alongcoast gradient over most of the region: thus, wintertime winds are not markedly different along the coast. Note that the weaker winter stress at the GH site is likely due to the fact that that site is relatively closer to shore where it can be affected by coastal topography. Wind stress from buoys [e.g., *Tinis et al.*, 2006] as well as scatterometer data (not shown) do not suggest marked weaker winds at midshelf off the Washington coast in winter. Therefore, wind stress data taken from a site at midshelf, ~40 km offshore of the coastline at the latitude of GH (labeled "GH40") are also included in winter in the analysis below.

Unlike winter wind stress, alongcoast structure in summertime upwelling-favorable wind stress is substantial, roughly a three-fold decrease south to north over the array every year (Figure 5a; see also the upwelling indices in Figure 1b). On the other hand, year to year amplitude variability is minimal: maximum equatorward wind stress was almost uniform for several years, with a noticeable decrease only in 2004 (Figure 5a). Overall, maximum summer upwelling-favorable wind stress is roughly 2–3 times weaker than maximum winter downwelling-favorable wind stress at all sites during the 5 year period studied (Figure 5a).

4.1.2. Timing of Seasonal Patterns

The timing of seasonal peaks in wind stress, water properties and alongshelf velocity differs substantially between seasons and, to a lesser extent, between years (Figure 5a). In winter, maximum downwelling-favorable wind stress usually occurs in the same month at all sites across the northern CCS. Maximum wind stress usually occurs in December or January, November 2001 being the only exception. Maximum poleward near surface velocity usually occurs in the same month as maximum poleward wind stress. Maximum

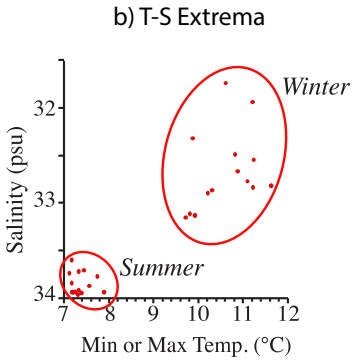

Figure 5b. T-S relationship for summer and winter near bottom, midshelf, water mass extrema.

wind stress generally occurs in the same month or one month prior to the appearance of the freshest and warmest water near bottom at midshelf.

In summer, as in winter, upwelling-favorable wind stress is usually strongest in the same month at all sites along the coast in a given year. Maximum upwelling-favorable wind stress generally occurs in June or July at all four sites. The coldest and saltiest water generally appears in July or August at the northern sites and June or even May at the southern sites. This 1–2 month south to north seasonal progression was also observed in 1981–1982 [*Strub et al*., 1987a]. Thus, in contrast to winter, summertime water properties reach their extremes at different times along the coast. At the northern two sites, as in winter, the strongest upwelling-favorable wind stress usually precedes the coldest, saltiest water or occurs in the same month as those extremes. At the southern two sites the coldest, saltiest water frequently leads upwelling-favorable wind stress (in 3/5 and 2/4 years at CB and RR, respectively). Maximum equatorward velocity occurs 1–3 months earlier than the maximum equatorward wind stress at most midshelf sites, thus leading near bottom water properties. The lead of shelf currents over local wind stress and temperature, first reported by *Hickey* [1979] for the CCS using large-scale data, was also observed with directly measured currents and temperatures in the annual cycle of mid water column midshelf temperatures in1981 and 1982 [*Strub et al*., 1987a].

4.1.3. Relationship Between Winds and Water Properties

Inspection of time series of wind stress and near bottom water properties suggests that the interannual variability in monthly averaged water property extremes is related to the strength of the alongshelf wind stress (Figure 5a). The variability in water properties is roughly three times greater in winter than in the upwelling season (Figure 5b). This result mirrors the variability in alongshelf wind stress at every location in our study site (Figure 6a); wind stress standard deviation is ~5 times greater in winter than in summer.

Downwelling-favorable wind stress increased for the first three winters, then decreased in winter 2003; water warmed and, with the exception of GH, freshened successively over the first three winters, then cooled and freshened in the final winter (2004) when downwelling-favorable wind stress weakened. In summer, near bottom temperatures and salinities were similar from year to year over the first four years when maximum upwelling-favorable wind stress was nearly constant; the upwelled bottom water freshened and warmed in summer 2004, when upwelling-favorable wind stress weakened. These relationships are explored further below using regressions and predicted variance. Since water properties in the majority of the water column are visually correlated to and in phase with near bottom water properties on both annual and interannual scales, the analysis uses near bottom water properties as a proxy for variability throughout the water column, with the exception of near surface layers influenced directly by the Columbia plume in winter and spring (GH and NH).

Interannual differences in water property extremes display a strong statistical relationship to local alongshelf wind stress at all sites in winter, with warmer temperatures under stronger downwelling-favorable wind stress (Figure 6a, top). A stronger relationship is observed between wind stress and temperature (predicted variance R^2 ~90% at 4 of 5 sites, and regression significance values exceed 75%; correlation coefficient R = 0.78–0.94) than between wind stress and salinity (R^2 = 28–72%, with significance values exceeding 50%; R = 0.53–0.85). Note that although confidence limits are relatively low in many cases due to low numbers of degrees of freedom, the pattern of regression slopes for temperature are similar at all sites along the coast, suggesting results are not due to random chance. Salinity relationships form roughly two groups: the wind stress-property relationship is offset along the salinity axis, with a prominent alongcoast gradient from north (fresher) to south (saltier) as expected due to the substantial poleward increase in freshwater.

Interannual differences in water property extremes in summer also display a relationship to local wind stress (R^2 = 14–76%, T; R^2 = 6–89%, S) (Figure 6a, middle). Slopes of both temperature and salinity regressions are

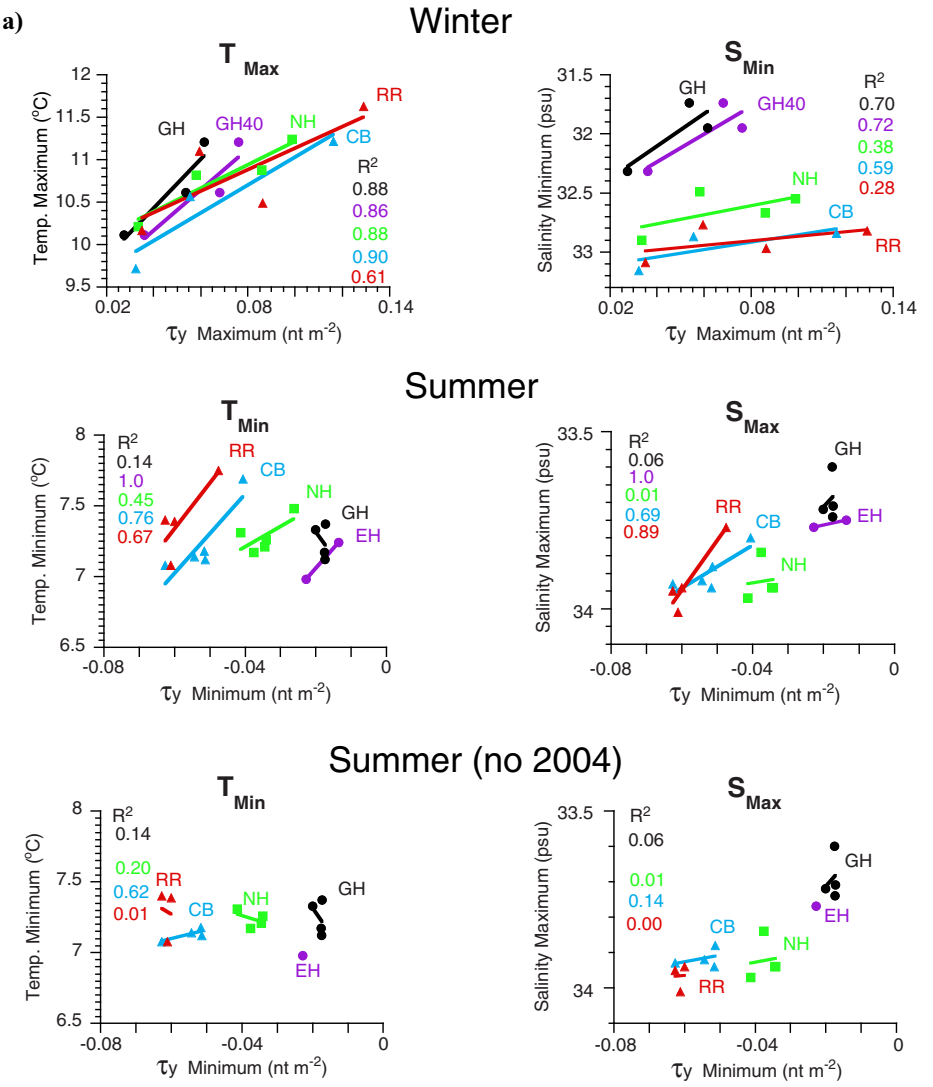

Figure 6a. Relationship between local alongshelf wind stress and near bottom temperature and salinity extremes in winter and summer at midshelf. The ratios of predicted to observed variance are given in the included key, printed north to south and color-coded to match the locations. Note similar regression slopes and variance for winter results at GH using winds extrapolated to the mooring location (GH) and winds 40 km offshore of the mooring (GH40). The bottom two plots are identical to the middle plots, except that data from 2004 were excluded from the analysis. Note the change to negative (downwelling-favorable) slopes for wind-temperature regressions at RR and NH when 2004 data were excluded.

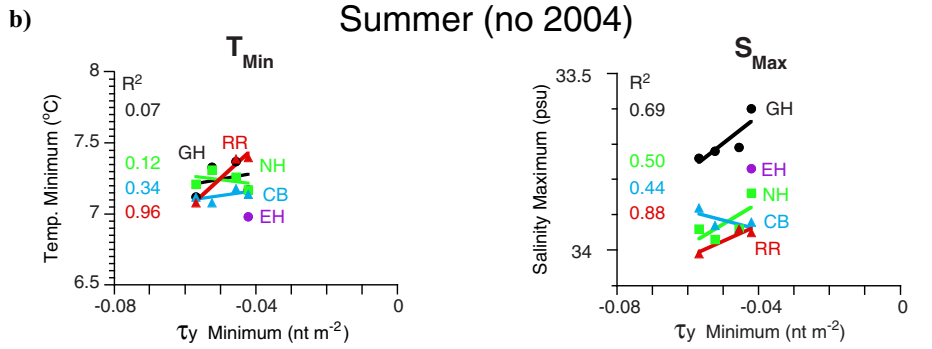

Figure 6b. Relationship between "remote" alongshelf wind stress and near bottom temperature and salinity extremes in summer at midshelf. Data from 2004 were excluded from the analysis. Wind stress data at 39°N ("remote stress") instead of wind stress data at the mooring sites ("local stress") were used in the analysis. The ratios of predicted to observed variance are given in the included key, printed north to south and color-coded to match the locations. Note the improvement in predicted variance for salinity at all sites and the reversal in the sign of the wind-temperature regressions to upwelling-favorable at most sites.

significant at more than the 50–90% level except at GH (both T and S) and NH (S only), with variance and confidence generally increasing equatorward for both properties. Stronger wind stress is associated with colder, more saline water at all sites, consistent with a local upwelling response. Regression slopes for both temperature and salinity are offset along the *x* axis, so that greater wind stress is needed equatorward to achieve the same decrease in temperature or increase in salinity.

Close inspection of Figures 5a and 6a shows that most of the predicted variance in summer is due primarily to the warming and freshening that occurred in 2004; in the first four years of the record, summertime near bottom water properties were virtually constant from year to year at each site and had no visual alongcoast trend. A straight line between the cluster of points for the first 3 years and the later years produces the seemingly strong linear relationship. Both temperature and salinity at sites with no data in 2004 (such as GH, T and S, and NH, S) have the weakest relationship with wind stress in summer (Figure 6a, middle). Regression with the year 2004 omitted (Figure 6a, bottom) yields extremely low predicted variances (less than 50% significance) for salinity ($R^2 = 0$–14%) and similarly for temperature ($R^2 \leq 20\%$ at 3 of 4 sites). Perhaps more telling, the wind stress-temperature regression has the wrong sign (negative) to be consistent with upwelling at three of the sites: warmer rather than colder water is related to greater upwelling-favorable wind stress, with the exception of CB.

The linear relationship between interannual differences in local wind stress and bottom water properties might suggest that local alongshelf wind stress is driving interannual changes in water properties. Indeed, as illustrated in Figure 5a, coastal wind stress variability is highly correlated in the northern CCS on interannual scales (correlations 0.94 for winter and 0.93 for summer between GH and RR sites, significant at the 95% level). However, although summertime wind stress differs by a factor of three across sites in all years, the interannual differences in water properties are similar each year among all sites; they are NOT proportional to local wind stress magnitude (e.g., the warmest near bottom water was observed toward the south where upwelling-favorable wind stress is stronger, not weaker). Nor are the water property trends indicative that background stratification substantially affects vertical displacement of isopycnals: stratification is weaker equatorward rather than poleward both on the shelf (Figure 2b) as well as farther seaward over the CCS (not shown; data from averages of World Ocean Database profiles offshore of 1000 m isobath out to 400 km from shore as used in *Connolly et al*. [2014]).

In the analysis above, wind stress was paired with water property extremes in two ways: using wind stress extremes in whatever month they occur (results shown in Figures 6a and 6b), and using wind stress extremes for the same month as the property extremes (not shown). In winter, the month of maximum wind stress did not appear to matter: predicted variance was similar in both cases. In summer, however, month did matter, with generally higher variance explained when maximum upwelling-favorable wind stress (regardless of month) was used. Note also that statistics worsened substantially when wind stress integrated over the upwelling season at each site was utilized (not shown).

4.2. Remote Forcing in the Northern CCS

Forcing by remote winds has frequently been shown to explain alongshelf current variability over CCS shelves on event time scales (e.g., [*Battisti and Hickey*, 1984; *Hickey*, 1984; *Hickey et al*., 2006] off central Washington; [*Chapman*, 1987; *Denbo and Allen*, 1987] off northern California; [*Hickey et al*., 2003; *Pringle and Riser*, 2003] off southern California). On seasonal scales, the rapid, whole coast transition from winter downwelling to spring upwelling conditions on the shelf [e.g., *Strub and James*, 1988] has been related in part to remote forcing over the shelf [*Strub et al*., 1987b]. Springtime equatorward transport on northern CCS shelves has been attributed to remote wind forcing [*Werner and Hickey*, 1983; *Pierce et al*., 2006]. Below we use our new data-based results and a model study to examine the degree to which remote forcing affects shelf water properties in the northern CCS on (1) seasonal and (2) interannual scales in winter and in summer.

The most remarkable result from the present data set is the large-scale nature of water upwelled from the upper slope onto the shelf in the upwelling season on both seasonal and interannual scales. Our results show that (1) near bottom water properties at midshelf below the surface layer are nearly identical over the ~450 km sampling array in summer in most years sampled, apparently impervious to mesoscale barriers such as Cape Blanco or submarine canyons, as well as to the ~3-fold latitudinal gradient in upwelling-favorable wind stress, variable stratification, shelf width and bottom slope. Also, (2) the slope of the wind

stress-property relationships as well as predicted variance differ substantially between winter and summer, consistent with dynamics differing seasonally (Figure 6a). In the winter downwelling season, predicted variance was extremely high and similar at all sites; a typical regression was T (°C) = 16.5 + 9.4 x Tauy (CB). In the summer upwelling season, variance was much weaker (Figure 6a) and the slope of the regressions was steeper (e.g., at CB, T (°C) = 8.7 + 28.0 × Tauy), indicating that almost twice the local wind stress is required to change water properties by the same amount as in winter. Lastly, (3) when 2004 data were removed from the water property time series (Figure 6a, bottom left), the near identical bottom temperature extremes in the first four upwelling seasons were associated with a wide range of local wind stress values, from the relatively weak ~ -0.02 nt m^{-2} at the most northern site to the relatively strong ~ -0.06 nt m^{-2} at the southern sites. These three results are all consistent with theoretical models of the CCS that invoke simple Kelvin wave or, more generally, coastally trapped wave dynamics and forcing by wind stress south of the region of interest ("remote" forcing) [e.g., *McCreary*, 1981; *Suginohara*, 1982; *Battisti and Hickey*, 1984; *Chapman*, 1987; *McCreary et al*., 1987; *Springer et al*., 2009; *Connolly et al*., 2014]. Some models include multiple wave modes, as well as realistic cross-margin topography and stratification. For example, *Chapman* [1987] found that two modes provide the best fit to alongshelf velocity over the northern California shelf; whereas *Connolly et al*. [2014] indicated four modes were optimal over the northern CCS (Juan de Fuca region) slope. Phase speeds averaged along the CCS coast were 387 and 73 cm s^{-1} for modes 1 and 4, respectively, in the *Connolly et al*. [2014] model. In all the models, the upwelling signal propagates poleward from the northern California coast, where seasonal upwelling-favorable wind stress is a maximum, to more northern regions, where upwelling-favorable wind stress is much weaker, uplifting local isopycnals without the need for local wind stress. Model studies also suggest that remotely forced signals may originate equatorward of the southern terminus of the CCS system on seasonal times scales [*Pares-Sierra and O'Brien*, 1989; *Connolly et al*., 2014].

The temperature and salinity interannual signals remaining in the summertime records after data from 2004 were removed are extremely small (compared to 2004) (Figure 6a). Moreover, regression with local wind stress produced relationships opposite that for upwelling. To evaluate whether any of the weak remaining interannual variability might be due to forcing by remote wind stress, we have recomputed regressions using wind stress from 39°N as a proxy for remote wind stress (Figure 6b).

Although predicted variance for temperature is less than that found using local winds at three of the four sites (7–34% at the three most northern sites, and 96% at the site closest to the forcing region; with significance levels $<$60% except at one site), use of remote wind stress does change the temperature-wind stress regression slope, producing the commonly expected upwelling relationship in which colder and saltier water is related to stronger wind stress. The fact that the appropriate pattern is produced is encouraging, if not definitive. The variance of salinity, in contrast to that of temperature, increases at all sites with the use of remote winds; significance is $>$50–80%. The different relationships shown by temperature and salinity are unexpected, and remain unclear.

Traditionally, correlation with wind stress equatorward of a region has been used as a proxy for identifying remote forcing. However all studies analyzed event rather than interannual scales [e.g., *Hickey et al*., 2003], or the shoreward progression of upwelling across the shelf within a single season [*Hickey et al*., 2006]. In fact, *Pringle and Riser* [2003] specifically conclude that no interannual relationship was found between temperature and remote winds. Our results suggest that another proxy, such as the alongshelf gradient in wind stress (see discussion of summer 2004 in section 4.3) might be more appropriate for interannual variability.

More definitive evidence for the importance of remote forcing in the upwelling season on seasonal scales is provided by a comparison of observed and modeled temperature sections, where a ROMS regional model (for details, see section 2 and also *Connolly and Hickey* [2014]), which includes disturbances propagating poleward into the northern CCS, is run with and without regional wind forcing over the northern CCS (Figure 7). Modeled and observed temperature sections across the central Washington shelf and upper slope ($\sim$47°N) are shown for exactly the same dates before and after the spring transition. The ROMS model is forced by regional winds, tides and surface heat fluxes, with boundary conditions prescribed from larger domain NCOM models that allow disturbances generated south of the regional domain to cross the southern boundary into the northern CCS. The spring section on 19 April was obtained 1 month prior to the estimated Pacific Northwest spring transition for 2005 (24 May) [*Kosro et al*., 2006]; the summer section on 19 July was obtained just subsequent to the onset of strong upwelling-favorable winds [e.g., *Hickey et al*., 2006;

Kosro et al., 2006]. In the early spring sections, both observed and modeled isotherms off the Washington coast show strong evidence of large-scale upwelling along the shelf bottom and below 150 m over the open slope (e.g., 7°C isotherm), even in the model run without any local winds (Figure 7). The colder upwelled water extends farther up the shelf bottom in the summer section, and as in spring, little difference is seen in model runs with and without local wind stress, except near the sea surface, where lack of wind-driven mixing and modification of surface heat flux are factors in the warmer-than-observed temperatures. Note that the near surface layer in the 19 April section, where modeled and observed isotherms have poorer agreement, is heavily influenced by the Columbia River plume at that time (see corresponding salinity sections in *Hickey et al*. [2013]). The *Connolly et al*. [2014] model does not include inflow from the Columbia plume.

In this scenario, large-scale remote forcing uplifts isopycnals all along the coast. In particular, in the northernmost CCS (Washington and northern Oregon) where local wind stress is one third that of northern California, remotely forced waves build the seasonal baroclinic structure of the CSS, including the poleward slope undercurrent and much of the shelf circulation. The resulting circulation moves this water shoreward across the shelf where local wind stress-driven upwelling can move it the sea surface within the internal Rossby radius of the coastline (∼10 km). For example, note how the 8°C water on 17 July extends closer to the coast in the model run that includes local wind stress.

Thus we conclude that remote forcing is critically important for setting up the summertime baroclinic circulation over the shelf and slope as postulated by authors such as *McCreary* [1981] decades ago. These dynamics set the basic water properties for annual properties upwelled onto the shelf. The variability of this pattern from year to year is minimal in our 5 year record in 4 out of 5 years. In the final year variability was more substantial, but still much less than wintertime year to year variability. Remote wind forcing is particularly effective in the CCS in summer, largely because alongshelf wind stress has a large alongcoast gradient in that season, setting the stage for the development of coastal trapped waves (Figures 1b and 5a). Remote wind forcing is not as important in winter months—coastal wind stress is more uniformly distributed in the CCS, or increases slightly poleward rather than equatorward (Figures 1b and 5a). This difference may help explain the previously discussed winter to summer differences in phase lags, correlations and wind/water property regressions.

4.3. Water Property Sources and Trends

Source waters for the shelves in the study region include the deep (150–500 m) poleward flowing warm, salty California Undercurrent, and the equatorward flowing, shallower (0–150 m) cold, fresh Subarctic water [*Hickey*, 1979]. Most studies have shown that the majority of near bottom shelf waters in this region are upwelled from the California Undercurrent [e.g., *MacFadyen et al*., 2008]. However, intrusions of Subarctic water onto the northern CCS shelves have occasionally been observed [*Huyer*, 2003]. One might therefore expect alongcoast trends in shelf water properties as a result of lateral advection of large-scale properties of the slope waters; "normal" large-scale trends are 2°C and 0.3 psu per 1000 km, warmer and saltier equatorward [*Huyer*, 2003]. In addition, an alongcoast trend (colder, saltier equatorward) might be expected from vertical advection due to the alongcoast increase in local upwelling-favorable wind stress toward the south. In spite of the above possibilities consistent alongcoast trends were not generally observed in the midshelf data sets in summer, 2004 being an exception, with warmer water equatorward (see details below) (Figure 6a, middle). In winter, a consistent alongcoast trend was observed only in salinity, reflecting the poleward increase of fresher water.

Measurable alongshelf near bottom gradients (∼0.2°C colder and 0.07 psu fresher poleward) were observed in the summers of 2003 and 2004 between northern Washington (EH2, where the coldest monthly mean temperature in our data set was measured) and central Oregon (NH) at midshelf in a similar bottom depth (Figure 3b), but this gradient did not consistently extend farther south. This trend might be due in part to local topography; in particular, the northern site is located just south of the Juan de Fuca canyon (see location in Figure 1a), a feature which enhances upwelling of deeper, colder water to the northern Washington shelf (see *Connolly and Hickey* [2014], Figure 6). Surface drifter tracks (see e.g., *MacFadyen et al*. [2005], Figure 5) as well as recent model studies [*Connolly and Hickey*, 2014] show that water upwelled in this region along the east-west trending canyon's southern edge flows equatorward from northern Washington to Oregon, thereby providing much of the bottom water to the northern CCS shelf.

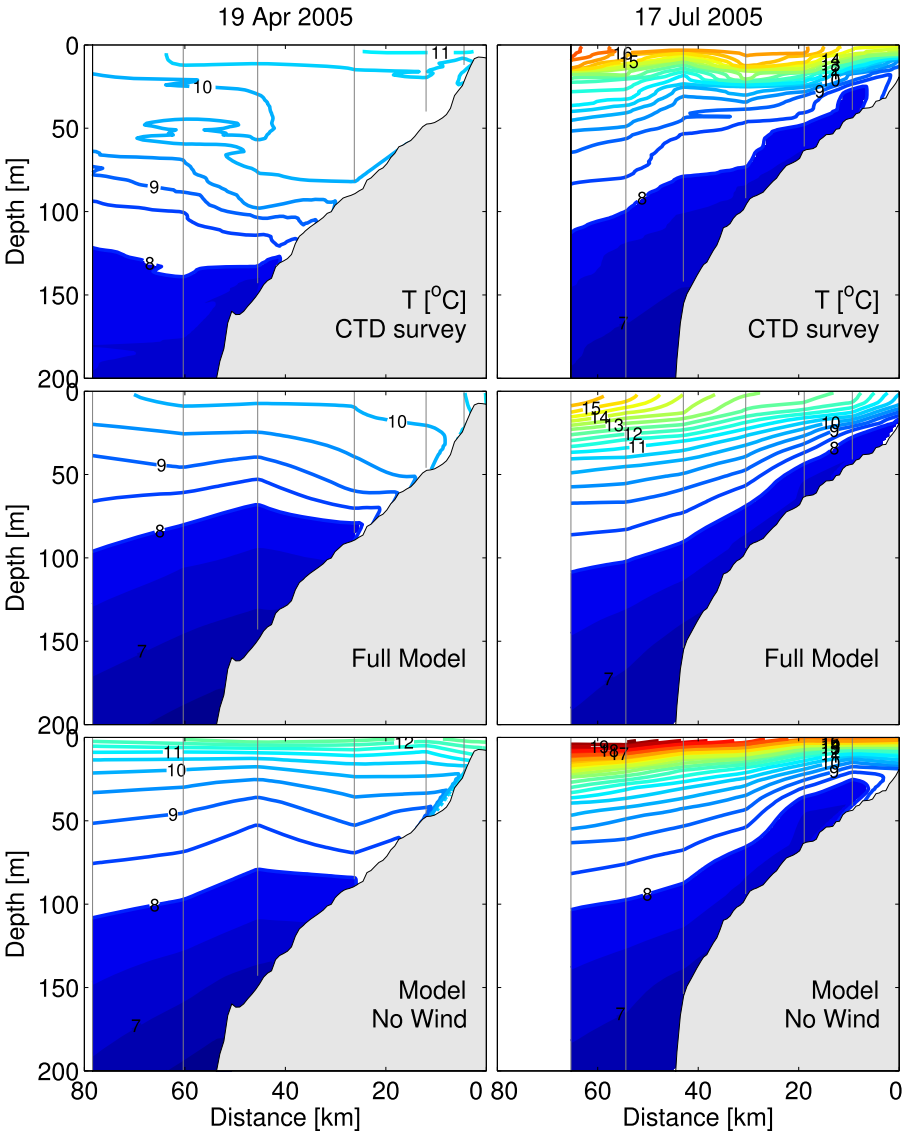

Figure 7. Observed and modeled temperature sections across the central Washington shelf and upper slope for selected dates in summer 2005. Individual stations subsampled for contouring are marked with vertical lines. The regional ROMS model was run with (Full Model) and without (No Wind) local wind forcing. Note the limited differences in water properties below the surface layers between the two cases. The regional model is set within a larger domain model of the entire CCS (NCOM-CCS on the southern boundary), allowing the passage of remotely forced waves into the regional model [*Connolly and Hickey*, 2014].

A substantial warming and freshening was observed at all sites in summer of 2004, with extreme temperatures and salinities that were fresher and warmer, respectively than all the preceding years at most sites (Figure 5a). Wind stress was also weaker in 2004 at all sites (Figure 5a), and the wind stress-water property relationships were strong at stations with 2004 data (67–89% of the variance, and >80% significance at the two southern stations, Figure 6a, middle). Thus it is tempting to explain the 2004 change in water properties as simply due to a decrease in wind stress resulting in reduced upwelling, rather than the result of alongcoast large-scale advection.

The 2004 warming actually began in 2003 at the southernmost site (RR), consistent with a change in either lateral advection or water properties of the southern water source. The greatest water property changes in 2004 relative to 2003 also occurred at the southern end of the study area (0.35°C, 0.18 psu at RR cf. 0.31°C at NH, 0.26°C, 0.02 psu at EH2). Although both the warming and the fact that it was greater and earlier to the south is consistent with enhanced poleward advection in the California Undercurrent, advection of Undercurrent water could only explain the freshening if the generally warmer, saltier Undercurrent also freshened.

CTD profiles from the northern CCS show that water in the core of the California Undercurrent water off the central Washington coast in 2004 was about 0.5°C warmer than is typical, and that fresher water was observed on the shelf because upwelling was shallower due to the weaker winds that year [*MacFadyen et al*., 2008]. Comparison of cross-shelf/slope sections of water properties obtained in Septembers of 2003–2006 from the central Washington coast (not shown) demonstrates that the depth of the undercurrent core (as indicated by the divergence of isopycnals, isotherms and isohalines) was shallower (~175 m) in 2004 than its typical depth of about 250 m [*Hickey*, 1979]. Moreover, the core of the Undercurrent was located above 26.5 σ_t, in contrast to its typical density, below 26.5 σ_t. Properties are consistent with upwelled water originating higher in the water column above the shoaled Undercurrent core, so that water of 7.5°C and 33.6–33.8 psu flooded most of the mid to outer shelf rather than the more typical 7.0–7.5°C and 33.9 psu observed in other years (not shown).

There is one scenario that is consistent with both the strong relationship to wind stress and changes in the Undercurrent core depth: this involves the partial collapse of remote forcing all along the US west coast. The alongcoast gradient in wind stress, critical to the development of coastal trapped waves, was weaker by at least one-half in 2004—the minimum in our 5 year record. The seasonal California Undercurrent would not readily develop in models without the alongcoast gradient in wind stress (see e.g., *McCreary* [1981]; *McCreary et al*. [1987]). Thus it is reasonable to conclude that Undercurrent properties would change substantially with a factor of two change in the alongcoast wind gradient. The remarkable collapse is confirmed in *Goericke et al*. [2005, Figure 4], which shows UI along the entire coast from 2001 to 2005. Only one other collapse is seen in a record of the Upwelling Indices from 996 to 2009 (not shown). Note that a much greater decrease in upwelling-favorable wind stress in 2004 occurred at the more southern latitudes: wind stress decreased by more than a factor of ten in comparison to a factor of ~2 in the north (UI amplitude decrease of 61% at 42°N versus 12% at 48°N). Thus the scenario involving a dramatic decrease in both coastal wind stress AND its alongcoast gradient, is also consistent with the observation that a larger effect occurs with water properties at the southern sites in 2004, those closest to the strongest wind forcing. In summary, the remarkable changes in 2004 are likely due to weakening in remote forcing (fewer and weaker coastally trapped waves, which affect both Undercurrent core depth and remotely forced upwelling) as well as local wind effects. Unfortunately our data are insufficient to definitively separate the two mechanisms.

4.4. Temporal Context of the Study Time Period

The properties of near bottom water upwelled at midshelf in summer remain remarkably constant for at least 3 years, and 4 years at some sites, then warm and freshen substantially. Because the record is relatively short, it is unclear whether the period of summertime near-constant properties of upwelled water or the period of warmer, fresher water is "anomalous" or whether the record as a whole is "typical."

In terms of water property values, summertime near bottom temperatures at the Washington and Oregon sites in the study period are comparable to seasonal extrema shown in the historical CTD-based literature [*Landry et al*., 1989]. For example, the coldest bottom temperatures off both Washington and Oregon at midshelf are ~7°C in the historical database, as observed in our time series; and the cold temperature at midshelf extends farther in time and higher in the water column off Washington than off Oregon, as also seen in the present data set (see Figure 3b).

To assess whether wind variability and magnitudes were typical of a longer time period (1996–2009), we considered a record of monthly average upwelling indices (UI) for a 14 year period that extends prior to and following our measurement period (not shown). Statistics were calculated for the strongest UI in each summer. At the southern end of the study region (42°N) these data display large UI over the first decade, with reduced values after 2003. The standard deviation at 42°N in the longer period is comparable to that in the study period (standard deviation 98 versus 85 $m^3\ s^{-1}$ per 100 m of coastline) and ranges are comparable. The standard deviation at 48°N in the study period is also comparable to that in the longer record (12.5 versus 11.1 $m^3\ s^{-1}$ per 100 m of coastline).

Although the large-scale winds in the study period thus appear to be reasonably representative of variability and structure over longer time periods using a statistical metric, it should be noted that 3 of the study years (2001, 2002, 2003) have the largest UI in the 14 year record and two years have winter winds at 39°N and 42°N almost as large as the 1997 El Niño. Also, the 2004 "collapse" of upwelling wind stress magnitude off southern Oregon and northern California and thus the alongcoast wind gradient was one of only two

such events in the 14 year record. The "State of the California Current" summary for 2004–2005 [*Goericke et al*., 2005] described 2004 as having only a "weak El Niño" and having reduced upwelling, but nothing particularly unusual was reported for that year.

In summary, the 2000–2004 period was not atypical of other periods. It includes a mild El Niño, an intrusion of Subarctic water [*Kosro*, 2003], several years of strong upwelling-favorable winds, and a year of weaker upwelling-favorable winds with a weaker alongcoast wind stress gradient. As suggested by our analysis, the year of weakest winds coincided with a change in slope water properties, possibly related to the partial "collapse" of remote forcing by wind stress and alteration of the undercurrent core depth. The forcing and responses are all typical of Eastern Boundary System variability. However, in the larger picture, because the Undercurrent core is rarely seen in historical data at the shallower depth and with lighter, fresher, warmer properties, we conclude that the 2004 upwelling season was less typical than the years of near constant upwelling-favorable wind stress and near uniform bottom water properties.

5. Conclusions

As a component of the GLOBEC Northeast Pacific program an array of moored sensors was maintained for 5 years along the northern CCS midshelf over an alongcoast distance of about 450 km. Fortuitously, the sample period included the typical seasonal ranges of both upwelling and downwelling-favorable wind stress amplitudes. The sensor array allowed analysis of both spatial and temporal patterns of variability on seasonal and interannual scales. Maximum upwelling-favorable wind stress decreases poleward by ~70% over the latitudinal range of the sensor array. The moorings spanned the area of influence of buoyant plumes from the Columbia River and other smaller coastal rivers, several submarine canyons, variable shelf width, stratification and bottom slope, as well as a coastal promontory where the southward coastal jet frequently separates from the shelf. The overriding conclusion is that *in spite of the substantial alongcoast trends in wind stress forcing and other physical differences along the coast*,

1. ***Seasonal properties of near bottom mid shelf waters are close to identical across the entire northern CCS in summer and in winter with no consistent alongcoast trends except in wintertime salinity*.**
2. ***Interannual variability of mid shelf water properties below the near surface, freshwater-influenced layers is similar across the entire northern CCS*.**

Water properties above the near bottom layers are modified by freshwater influx**,** which produces strong alongcoast gradients in salinity, density and stratification variability (fresher, lighter, more stratified to the north). In the most northern latitudes, sea surface and subsurface temperatures are almost perfectly out of phase seasonally, a result of direct and indirect freshwater-influenced effects. In addition, a three layer temperature profile occurs in winter and early spring at the two northern sites. Thus sea surface temperature data cannot generally be used in the northern CCS to extrapolate features downward into the deeper water column as has been done using satellite data; nor can sea surface temperature data from moored sensors such as NDBC buoys be used alone to validate models or extrapolate backward in time below near surface layers.

Unlike water properties, alongshelf near surface velocity at mid shelf is not large scale, displaying measurable alongcoast differences between each site, and no consistent alongcoast trends. Also, no consistent relationship between wind stress and year-to-year velocity differences was observed. However, variability related to actual interannual changes in velocity and those due to cross-shelf movement of the coastal jet could not be distinguished with this data set.

The 5 year record and a regional model study allowed analysis of the relationship between annual water property extremes and wind stress forcing, both local and remote. Results demonstrate that:

1. ***Wintertime and summertime alongcoast patterns of water property variation have distinctly different relationships to wind stress variability and its alongcoast structure*.**

In winter, year-to-year temperature extremes at midshelf are highly variable, and strongly related to alongshelf wind stress variability. However, because wind stress itself is very large scale, subsurface temperatures are relatively uniform along the coast. Summertime patterns are the opposite of those in winter: wind stress and water properties have much less variability from year to year and water properties vary minimally and

are only weakly related to local wind stress, 2004 being the exception. Unlike winter, alongcoast wind stress structure is significant (~a 3-fold gradient), and temperature trends, when observed, generally opposed the wind stress trend: colder temperatures were observed in regions with weaker winds.

The large-scale nature of the measured summertime water properties reinforce the theoretical idea that coastal trapped wave dynamics are of order one importance to upwelling dynamics in the northern CCS. For example, remote forcing by winds ~800 km south of the northernmost mooring site predicted salinity variation at the most northern sites better than local wind stress and, unlike local stress, produced a temperature-wind stress regression with the correct slope for upwelling dynamics at most sites. The remote forcing, although responsible for much of the overall seasonal properties of northern CCS waters, caused little year to year variability of the summertime water properties, in all but one of the five record years.

The one year in which alongcoast subsurface water property trends were observed (2004) was unusual in that warmer, fresher water was observed at all sites, the largest property changes occurred in the southern part of the study area, and that year was the only year when a consistent alongcoast trend was observed in near bottom temperatures (warmer to the south). Our analysis was consistent with the observation that the core of the slope poleward Undercurrent was shallower, warmer and fresher that year in the northern CCS. Numerous theoretical and numerical model studies demonstrate that the Undercurrent is a remotely generated, whole coast feature, related to coastal trapped wave dynamics, and dependent on the alongcoast gradient in wind stress. We suggest the shallower core depth is a result of the partial collapse of the large-scale alongcoast wind gradient as well as the weakening of wind stress all along the coast. Thus, both weaker remote and local winds and the loss of the alongcoast wind stress gradient that builds the remote forcing response along the CCS, including the Undercurrent, likely contributed to the unusual water properties that year.

Many of the important results are a direct result of the importance of remote forcing in the CCS. The CCS is characterized by an alongshelf wind stress field that is remarkably coherent along the coast, in a region with a relatively long straight coastline and continental shelf edge, the near perfect wave guide. In summer (but not in winter) wind stress has a large alongcoast gradient, with maximum strength south of the northern CCS, which leads to the generation of coastally trapped poleward propagating waves. Thus, it is not surprising that remote forcing plays a prominent role in spring to summertime seasonal dynamics in the northern CCS. Yet, in the past few decades, with the advent of regional models, remote forcing was often downplayed in the CCS in favor of more local processes, instabilities, regional topography and eddies. As models have grown in skill, resolution and spatial extent, scientists have again become cognizant of the importance of carefully including remotely driven energy entering through equatorward model boundaries at all temporal scales [e.g., *Springer et al*., 2009; *Giddings et al*., 2014]. It is our hope that as we move to ever more comprehensive and useful models of the coastal ocean, the phase and spatial and temporal relationships deduced from the remarkable, difficult-to-obtain data set presented herein will provide important benchmarks for model testing, as well as encourage examination and interpretation of the new data sets that will become available though the new ocean observing networks in the coming decades.

Acknowledgments

Mooring data collection was supported by the National Science Foundation (OCE0001034, OCE0234587 to B. Hickey and OCE0000733, OCE0434810 to M. Kosro) and by the Coastal Ocean Program of the National Atmospheric and Oceanic Administration (NOAA) (NA17OP2789 to B. Hickey, MOA-2000-307 to S. Ramp, and OCE0237710, NA03NES4400001 and NA11NOS0120036 to P. M. Kosro). Analysis was supported by these grants as well as NA17RJ1232, NA09NOS4780180, OCE0942675, OCE1332753 to B. Hickey. The support of Beth Turner of the GLOBEC program is gratefully acknowledged. NCEP Reanalysis data were provided by NOAA/OAR/ESRL PSD, Boulder, Colorado, USA, from their Web site at http://www.esrl.noaa.gov/psd/. CTD data collection was supported by ECOHAB PNW and ORHAB (NOAA Coastal Ocean Program, NA07OA0310 grant to B. Hickey). These data are available at the Biological and Chemical Data Management Office (BCO-DMO). Mooring data are publicly available (locations GH and CB, contact B. Hickey at bhickey@u.washington.edu; NH10 at BCO-DM; RR at the National Oceanographic Data Center (NODC)). This is contribution #754 of the US GLOBEC program and #ECO867 and 15, respectively, 15 of the ECOHAB and PNWTOX programs. The findings and conclusions are those of the authors and do not necessarily reflect those of NSF, NOAA or the Department of Commerce. The authors would like to thank the sea going research teams of GLOBEC, ECOHAB PNW and ORHAB, in particular, W. Fredericks, J. Johnson, T. Juhasz, M. Stone, and W. Waldorf for their roles in data collection.

References

Allen, J. S., P. A. Newberger, and J. Federiuk (1995), Upwelling circulation on the Oregon continental shelf. Part I. Response to idealized forcing, *J. Phys. Oceanogr.*, *25*, 1843–1865.

Bakun, A. (1975), Daily and weekly upwelling indices, west coast of North America, 1967–1973, *NOAA Tech. Rep. 16, NMFS-SSRF-693*, 114 pp., U.S. Dep. of Commer., Washington, D. C.

Barnes, C. A., A. C. Duxbury, and B. A. Morse (1972), Circulation and selected properties of the Columbia River effluent at sea, in *The Columbia River Estuary and Adjacent Ocean Waters*, edited by A. T. Pruter and D. L. Alverson, pp. 41–80, Univ. of Wash. Press, Seattle.

Barth, J. A., S. D. Pierce, and R. L. Smith (2000), A separating coastal upwelling jet at Cape Blanco, Oregon and its connection to the California Current System, *Deep Sea Res., Part II*, *47*, 783–810, doi:10.1016/S0967-0645(99)00127-7.

Battisti, D. S., and B. M. Hickey (1984), Application of remote wind-forced coastal trapped wave theory to the Oregon and Washington coasts, *J. Phys. Oceanogr.*, *14*, 887–903, doi:10.1175/1520-0485(1984)014<0887:AORWFC>2.0.CO;2.

Chapman, D. C. (1983), On the influence of stratification and continental shelf and slope topography on the dispersion of subinertial coastally trapped waves, *J. Phys. Oceanogr.*, *13*(9), 1641–1652.

Chapman, D. C. (1987), Application of wind-forced, long, coastal-trapped wave theory along the California coast, *J. Geophys. Res.*, *92*(C2), 1798–1816, doi:10.1029/JC092iC02p01798.

Connolly, T. P., and B. M. Hickey (2014), Regional impact of submarine canyons during seasonal upwelling, *J. Geophys. Res. Oceans*, *119*, 953–975, doi:10.1002/2013JC009452.

Connolly, T. P., B. M. Hickey, I. Shulman, and R. E. Thomson (2014), Coastal trapped waves, alongshore pressure gradients, and the California Undercurrent, *J. Phys. Oceanogr.*, *44*, 319–342, doi:10.1175/JPO-D-13-095.1.

Denbo, D. W., and J. S. Allen (1987), The large-scale response to atmospheric forcing of shelf currents and coastal sea level off the west coast of North America: May–July 1981 and 1982, *J. Geophys. Res.*, *92*(C2), 1757–1782, doi:10.1029/JC092iC02p01861.
Fairall, C. W., E. F. Bradley, J. E. Hare, A. A. Grachev, and J. B. Edson (2003), Bulk parameterization of air-sea fluxes: Updates and verification for the COARE algorithm, *J. Clim.*, *16*, 571–591.
Foreman, M. G. G., W. R. Crawford, J. Y. Cherniawsky, R. F. Henry, and M. R. Tarbotton (2000), A high-resolution assimilating tidal model for the northeast Pacific Ocean, *J. Geophys. Res.*, *105*(C12), 28,629–28,651, doi:10.1029/1999JC000122.
Freeland, H. J., and K. L. Denman (1982), A topographically controlled upwelling center off southern Vancouver Island, *J. Mar. Res.*, *40*, 1069–1093.
García-Berdeal, I., B. M. Hickey, and M. Kawase (2002), Influence of wind stress and ambient flow on a high discharge river plume, *J. Geophys. Res. Oceans*, *107*(C9), 3130, doi:10.1029/2001JC000932.
Giddings, S. N., P. MacCready, B. M. Hickey, N. S. Banas, K. A. Davis, S. A. Siedlecki, V. L. Trainer, R. M. Kudela, N. A. Pelland, and T. P. Connolly (2014), Hindcasts of potential harmful algal bloom transport pathways on the Pacific Northwest coast, *J. Geophys. Res. Oceans*, *119*, 2439–2461, doi:10.1002/2013JC009622.
Goericke, R., et al. (2005), The state of the California Current, 2004–2005: Still cool? *CALCOFI Rep.*, *46*, pp. 32–71, Scripps Inst. of Oceanogr., San Diego, Calif.
Haugerud, R. A. (1999), Digital elevation model (DEM) of Cascadia, latitude 39N–53N, longitude 116W–133W, *Open File Rep. 99-369*, U.S. Geol. Surv., Reston, Va.
Hickey, B. M. (1979), The California current system—hypotheses and facts, *Prog. Oceanogr.*, *8*, 191–279, doi:10.1016/0079-6611(79)90002-8.
Hickey, B. M. (1984), The fluctuating longshore pressure gradient on the Pacific Northwest shelf: A dynamical analysis, *J. Phys. Oceanogr.*, *14*(2), 276–293.
Hickey, B. M. (1989), Patterns and processes of circulation over the Washington continental shelf and slope, in *Coastal Oceanography of Washington and Oregon*, edited by M. R. Landry and B. M. Hickey, pp. 41–115, Elsevier, Amsterdam, Netherlands.
Hickey, B. M. (1998), Coastal Oceanography of Western North America from the tip of Baja California to Vancouver Island, in *The Sea*, vol. 11, edited by K. H. Brink and A. R. Robinson, pp. 345–393, John Wiley, N. Y.
Hickey, B. M., and N. S. Banas (2003), Oceanography of the U.S. Pacific Northwest coastal ocean and estuaries with application to coastal ecology, *Estuaries*, *26*(4), 1010–1031, doi:10.1007/BF02803360.
Hickey, B. M., and N. S. Banas (2008), Why is the Northern California Current System so productive?, *Oceanography*, *21*(4), 90–107, doi:10.5670/oceanog.2008.07.
Hickey, B. M., L. J. Pietrafesa, D. A. Jay, and W. C. Boicourt (1998), The Columbia River Plume Study: Subtidal variability of the velocity and salinity fields, *J. Geophys. Res.*, *103*(C5), 10,339–10,368, doi:10.1029/97JC03290.
Hickey, B. M., E. L. Dobbins, and S. E. Allen (2003), Local and remote forcing of currents and temperature in the central Southern California Bight, *J. Geophys. Res.*, *108*(C3), 3081, doi:10.1029/2000JC000313.
Hickey, B., S. Geier, N. Kachel, and A. MacFadyen (2005), A bi-directional river plume: The Columbia in summer, *Cont. Shelf Res.*, *25*, 1631–1656, doi:10.1016/j.csr.2005.04.010.
Hickey, B., A. MacFadyen, W. Cochlan, R. Kudela, K. Bruland, and C. Trick (2006), Evolution of chemical, biological, and physical water properties in the northern California Current in 2005: Remote or local wind forcing?, *Geophys. Res. Lett.*, *33*, L22S02, doi:10.1029/2006GL026782.
Hickey, B., R. McCabe, S. Geier, E. Dever, and N. Kachel (2009), Three interacting freshwater plumes in the northern California Current System, *J. Geophys. Res.*, *114*, C00B03, doi:10.1029/2008JC004907.
Hickey, B. M., et al. (2010), River Influences on Shelf Ecosystems: Introduction and synthesis, *J. Geophys. Res.*, *115*, C00B17, doi:10.1029/2009JC005452.
Hickey, B. M., V. L. Trainer, P. M. Kosro, N. G. Adams, T. P. Connolly, N. B. Kachel, and S. L. Geier (2013), A springtime source of toxic *Pseudo-nitzschia* cells on razor clam beaches in the Pacific Northwest, *Harmful Algae*, *25*, 1–14, doi:10.1016/j.hal.2013.01.006.
Huyer, A. (1983), Coastal upwelling in the California current system, *Prog. Oceanogr.*, *12*, 259–284, doi:10.1016/0079-6611(83)90010-1.
Huyer, A. (1990), Shelf circulation, in *The Sea*, Ocean Eng. Sci., vol. 9, edited by B. Le Mehaute and D. M. Hanes, pp. 423–466, John Wiley, N. Y.
Huyer, A. (2003), Preface to special section on enhanced Subarctic influence on the California Current, 2002, *Geophys. Res. Lett.*, *30*(15), 8019, doi:10.1029/2003GL017724.
Huyer, A., P. M. Kosro, S. J. Lentz, and R. C. Beardsley (1989), Poleward flow in the California Current system, in *Poleward Flows Along Eastern Ocean Boundaries, Coastal Estuarine Stud. 34*, edited by S. Neshyba et al., pp. 142–159, Springer, N. Y.
Huyer, A., J. H. Fleischbein, J. Keister, P. M. Kosro, N. Perlin, R. L. Smith, and P. A. Wheeler (2005), Two coastal upwelling domains in the northern California Current system, *J. Mar. Res.*, *63*(5), 901–929, doi:10.1357/002224005774464238.
Huyer, A., P. A. Wheeler, P. T. Strub, R. L. Smith, R. Letelier, and P. M. Kosro (2007), The Newport line off Oregon–Studies in the North East Pacific, *Prog. Oceanogr.*, *75*(2), 126–160, doi:10.1016/j.pocean.2007.08.003.
Kalnay, E., et al. (1996), The NCEP/NCAR 40-year Reanalysis Project, *Bull. Am. Meteorol. Soc.*, *77*(3), 437–471, doi:10.1175/1520-0477(1996)077 < 0437:TNYRP>2.0.CO;2.
Kara, A. B., C. N. Barron, P. J. Martin, L. F. Smedstad, and R. C. Rhodes (2006), Validation of interannual simulations from the 1/8 degree global Navy Coastal Ocean Model (NCOM), *Ocean Modell.*, *11*(3), 376–398, doi:10.1016/j.ocemod.2005.01.003.
Kosro, P. M. (2002), A poleward jet and an equatorward undercurrent observed off Oregon and northern California during the 1997–98 El Niño, *Prog. Oceanogr.*, *54*(1–4), 343–360, doi:10.1016/S0079-6611(02)00057-5.
Kosro, P. M. (2003), Enhanced southward flow over the Oregon shelf in 2002: A conduit for subarctic water, *Geophys. Res. Lett.*, *30*(15), 8023, doi:10.1029/2003GL017436.
Kosro, P. M. (2005), On the spatial structure of coastal circulation off Newport, Oregon, during spring and summer 2001 in a region of varying shelf width, *J. Geophys. Res.*, *110*, C10S06, doi:10.1029/2004JC002769.
Kosro, P. M., W. T. Peterson, B. M. Hickey, R. K. Shearman, and S. D. Pierce (2006), Physical versus biological spring transition: 2005, *Geophys. Res. Lett.*, *33*, L22S03, doi:10.1029/2006GL027072.
Kudela, R. M., W. P. Cochlan, T. D. Peterson, and C. G. Trick (2006), Impacts of phytoplankton biomass and productivity in the Pacific Northwest during the warm ocean conditions of 2005, *Geophys. Res. Lett.*, *33*, L22S06, doi:10.1029/2006GL026772.
Landry, M. R., J. R. Postel, W. K. Peterson, and J. Newman (1989), Broad-scale distributional patterns of hydrographic variables on the Washington/Oregon shelf, in *Coastal Oceanography of Washington and Oregon*, edited by M. R. Landry and B. M. Hickey, pp. 1–40, Elsevier, Amsterdam, Netherlands.
Large, W. G., and S. Pond (1981), Open ocean momentum flux measurements in moderate to strong winds, *J. Phys. Oceanogr.*, *11*, 324–336, doi:10.1175/1520-0485(1981)01 < 0324:OOMFMI>2.0.CO;2.
MacFadyen, A., B. M. Hickey, and M. G. G. Foreman (2005), Transport of surface waters from the Juan de Fuca eddy region to the Washington coast, *Cont. Shelf Res.*, *25*(16), 2008–2021, doi:10.1016/j.csr.2005.07.005.
MacFadyen, A., B. M. Hickey, and W. P. Cochlan (2008), Influences of the Juan de Fuca Eddy on circulation, nutrients, and phytoplankton production in the northern California Current System, *J. Geophys. Res.*, *113*, C08008, doi:10.1029/2007JC004412.

Mass, C. F., et al. (2003), Regional environmental prediction over the Pacific Northwest, *Bull. Am. Meteorol. Soc.*, *84*(10), 1353–1366, doi:10.1175/BAMS-84-10-1353.
Mazzini, P. L. F., J. A. Barth, R. K. Shearman, and A. Erofeev (2014), Buoyancy-driven coastal currents off Oregon during fall and winter, *J. Phys. Oceanogr.*, *44*, 2854–2876, doi:10.1175/JPO-D-14-0012.1.
McCreary, J. P. (1981), A linear stratified ocean model of the coastal undercurrent, *Philos. Trans. R. Soc. London A*, *30*, 385–413.
McCreary, J. P., P. K. Kundu, and S. Chao (1987), On the dynamics of the California Current system, *J. Mar. Res.*, *45*(1), 1–32, doi:10.1357/002224087788400945.
McGary, N. B. (1971), An atlas of the Columbia river effluent and its distribution at sea, *Univ. Wash. Spec. Rep. 47*, 57 pp.
Pares-Sierra, A., and J. J. O'Brien (1989), The seasonal and interannual variability of the California Current system: A numerical model, *J. Geophys. Res.*, *94*(C3), 3159–3180, doi:10.1029/JC094iC03p03159.
Pierce, S. D., R. L. Smith, P. M. Kosro, J. A. Barth, and C. D. Wilson (2000), Continuity of the poleward undercurrent along the eastern boundary of the mid-latitude north Pacific, *Deep Sea Res., Part II*, *47*, 811–829, doi:10.1016/S0967-0645(99)00128-9.
Pierce, S. D., J. A. Barth, R. E. Thomas, and G. W. Fleischer (2006), Anomalously warm July 2005 in the northern California Current: Historical context and the significance of cumulative wind stress, *Geophys. Res. Lett.*, *33*, L22S04, doi:10.1029/2006GL027149.
Pringle, J. M., and K. Riser (2003), Remotely forced nearshore upwelling in Southern California, *J. Geophys. Res.*, *108*(C4), 3131, doi:10.1029/2002JC001447.
Ramp, S. R., and F. L. Bahr (2008), Seasonal evolution of the upwelling process south of Cape Blanco, *J. Phys. Oceanogr.*, *38*(1), 3–28, doi:10.1175/2007JPO3345.1.
Shchepetkin, A. F., and J. C. McWilliams (2005), The regional oceanic modeling system (ROMS): A split-explicit, free-surface, topography-following-coordinate oceanic model, *Ocean Modell.*, *9*(4), 347–404, doi:10.1016/j.ocemod.2004.08.002.
Shulman, I., J. C. Kindle, S. deRada, S. C. Anderson, B. Penta, and P. J. Martin (2004), Development of a hierarchy of nested models to study the California Current system, in *8th International Conference on Estuarine and Coastal Modeling 2003*, edited by M. L. Spaulding, pp. 74–87, Am. Soc. of Civ. Eng., Reston, Va.
Song, Y., and D. Haidvogel (1994), A semi-implicit ocean circulation model using a generalized topography-following coordinate system, *J. Comput. Phys.*, *115*(1), 228–244, doi:10.1006/jcph.1994.1189.
Springer, S. R., R. M. Samelson, J. S. Allen, G. D. Egbert, A. L. Kurapov, R. N. Miller, and J. C. Kindle (2009), A nested grid model of the Oregon Coastal Transition Zone: Simulations and comparisons with observations during the 2001 upwelling season, *J. Geophys. Res.*, *114*, C02010, doi:10.1029/2008JC004863.
Strub, P. T., and C. James (1988), Atmospheric conditions during the spring and fall transitions in the coastal ocean off western United States, *J. Geophys. Res.*, *93*(C12), 15,561–15,584, doi:10.1029/JC093iC12p15561.
Strub, P. T., J. S. Allen, A. Huyer, R. L. Smith, and R. C. Beardsley (1987a), Seasonal cycles of currents, temperatures, winds and sea level over the northeast Pacific continental shelf: 35°N to 48°N, *J. Geophys. Res.*, *92*(C2), 1507–1526, doi:10.1029/JC092iC02p01507.
Strub, P. T., J. S. Allen, A. Huyer, and R. L. Smith (1987b), Large-scale structure of the spring transition in the coastal ocean off western North America, *J. Geophys. Res.*, *92*(C2), 1527–1544, doi:10.1029/JC092iC02p01527.
Suginohara, N. (1982), Coastal upwelling: Onshore-offshore circulation, equatorward coastal jet and poleward undercurrent over a continental shelf-slope, *J. Phys. Oceanogr.*, *12*, 272–284, doi:10.1175/1520-0485(1982)01 < 0272:CUOCEC > 2.0.CO;2.
Sutherland, D. A., P. MacCready, N. S. Banas, and L. F. Smedstad (2011), A model study of the Salish Sea estuarine circulation, *J. Phys. Oceanogr.*, *41*, 1125–1143.
Thomson, R. E., and M. V. Krassovski (2010), Poleward reach of the California Undercurrent extension, *J. Geophys. Res.*, *115* C09027, doi:10.1029/2010JC006280.
Tinis, S. W., R. E. Thomson, C. F. Mass, and B. M. Hickey (2006), Comparison of MM5 and meteorological buoy winds from British Columbia to Northern California, *Atmos. Ocean*, *44*(1), 65–81, doi:10.3137/ao.440105.
Werner, F. E., and B. M. Hickey (1983), The role of a longshore pressure gradient in Pacific Northwest coastal dynamics, *J. Phys. Oceanogr.*, *13*, 395–410, doi:10.1175/1520-0485(1983)01 < 0395:TROALP > 2.0.CO;2.